Tectonophysics 665 (2015) 236–250

Contents lists available at ScienceDirect

Tectonophysics

journal homepage: www.elsevier.com/locate/tecto

Constraints on deformation of the Southern Andes since the Cretaceous from anisotropy of magnetic susceptibility

Marco Maffione [a,*], Catalina Hernandez-Moreno [b], Matias C. Ghiglione [c], Fabio Speranza [b], Douwe J.J. van Hinsbergen [a], Emanuele Lodolo [d]

[a] Department of Earth Sciences, Utrecht University, Utrecht, Netherlands
[b] Istituto Nazionale di Geofisica e Vulcanologia, Rome, Italy
[c] Instituto de Estudios Andinos "Don Pablo Groeber", Universidad de Buenos Aires–CONICET
[d] Istituto Nazionale di Oceanografia e di Geofisica Sperimentale (OGS), Trieste, Italy

ARTICLE INFO

Article history:
Received 13 May 2015
Received in revised form 23 August 2015
Accepted 4 October 2015
Available online 21 October 2015

Keywords:
Patagonian Orocline
Tectonics
Southern Andes
Anisotropy of magnetic susceptibility
Cordillera Darwin

ABSTRACT

The southernmost segment of the Andean Cordillera underwent a complex deformation history characterized by alternation of contractional, extensional, and strike-slip tectonics. Key elements of southern Andean deformation that remain poorly constrained, include the origin of the orogenic bend known as the Patagonian Orocline (here renamed as Patagonian Arc), and the exhumation mechanism of an upper amphibolite facies metamorphic complex currently exposed in Cordillera Darwin. Here, we present results of anisotropy of magnetic susceptibility (AMS) from 22 sites in Upper Cretaceous to upper Eocene sedimentary rocks within the internal structural domain of the Magallanes fold-and-thrust belt in Tierra del Fuego (Argentina). AMS parameters from most sites reveal a weak tectonic overprint of the original magnetic fabric, which was likely acquired upon layer-parallel shortening soon after sedimentation. Magnetic lineation from 17 sites is interpreted to have formed during compressive tectonic phases associated to a continuous ~ N-S contraction. Our data, combined with the existing AMS database from adjacent areas, show that the Early Cretaceous-late Oligocene tectonic phases in the Southern Andes yielded continuous contraction, variable from ~ E-W in the Patagonian Andes to ~ N-S in the Fuegian Andes, which defined a radial strain field. A direct implication is that the exhumation of the Cordillera Darwin metamorphic complex occurred under compressive, rather than extensional or strike-slip tectonics, as alternatively proposed. If we agree with recent works considering the curved Magallanes fold-and-thrust belt as a primary arc (i.e., no relative vertical-axis rotation of the limbs occurs during its formation), then other mechanisms different from oroclinal bending should be invoked to explain the documented radial strain field. We tentatively propose a kinematic model in which reactivation of variably oriented Jurassic faults at the South American continental margin controlled the Late Cretaceous to Cenozoic evolution of the Magallanes fold-and-thrust belt, yielding the observed deformation pattern.

1. Introduction

The Andean Cordillera is considered the archetype of non-collisional orogens, as it formed above a subduction zone consuming oceanic lithosphere of the Nazca (Farallon), Phoenix (Aluk), and Antarctic plates below the South American plate (e.g., Jordan et al., 1983; Ramos, 1999; Ramos et al., 2014). This process resulted in an orogenic system 200 to 700 km wide, spanning the South American continent from ~7°N to ~56°S. The present-day tectonic setting of the Andes is characterized by mainly eastward verging basement thrusts in the hinterland that transfer shortening to the fold-and-thrust belt (e.g., Espurt et al., 2011). In the central and southern sectors of the Cordillera two regional-scale orogenic arcs occur, identified by a significant curvature of the main structural trends. The northern one (14°-26°S), known as the Bolivian Orocline (e.g., Eichelberger et al., 2013; Isacks, 1988), is a secondary orocline (sensu Weil and Sussman, 2004) formed by opposite-sense vertical-axis rotation of the two limbs (e.g., Eichelberger et al., 2013; Maffione et al., 2009; Prezzi et al., 2014). More controversial is the tectonic history and style of deformation that controlled the origin of the orogenic re-entrant named as the 'Patagonian Orocline' by Carey (1958) at the southernmost tip of the Andean Cordillera (Fig. 1). Here, the ~ N–S-trending southern Patagonian Andes and the ~ ESE–WNW-trending Fuegian Andes define an orogenic curvature with an interlimb angle of ~110° (Kraemer, 2003). Source of uncertainty on the tectonic evolution of the Southern Andes is due to multiple interaction, where the South American plate underwent convergence with the Antarctic, Phoenix, and Nazca plates to the south and west, and divergence with

* Corresponding author.
E-mail address: m.maffione@uu.nl (M. Maffione).

http://dx.doi.org/10.1016/j.tecto.2015.10.008
0040-1951/

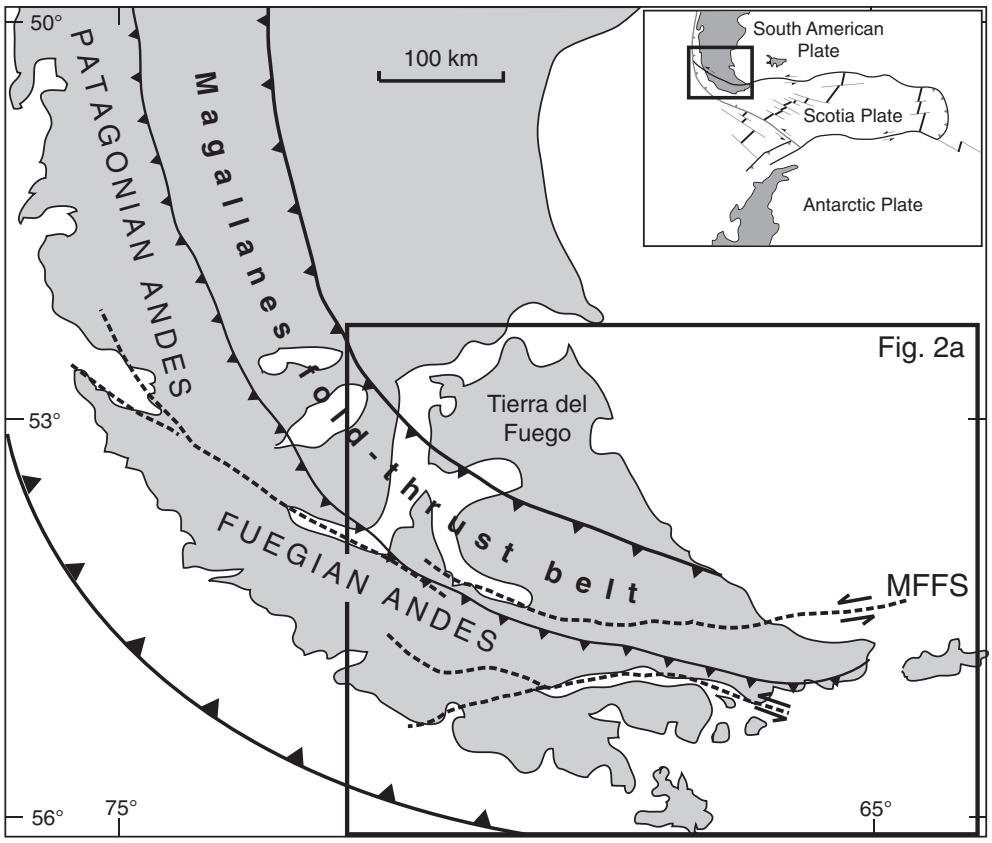

Fig. 1. Simplified tectonic setting of the Southern Andes showing the main tectonic features and structural domains.

the Antarctic and, later, the Scotia plate in the southeast. This complex geodynamic setting yielded alternation of extensional, strike-slip, and compressive events from the Jurassic until the late Cenozoic (Klepeis and Austin, 1997).

Early models considered the curved segment of the Southern Andes as a true orocline (*sensu* Weil and Sussman, 2004), interpreting its formation as due to bending of an originally straight orogen accompanied by large-scale counterclockwise rotation of the southern limb of the arc throughout the Cretaceous and Cenozoic (e.g., Carey, 1958; Dalziel et al., 1973; Kraemer, 2003). Other models explained the curvature of the Southern Andes by invoking strike-slip and transpressional tectonics (Cunningham, 1993) segmenting the southern tip of the Andean cordillera since the Late Cretaceous but without producing significant tectonic rotations. Other authors suggested that oroclinal bending occurred during the initial (Cretaceous) tectonic phases of the Andean orogeny associated with the closure of the Rocas Verdes marginal basin, but it ceased afterwards (Burns et al., 1980). More recently, a primary origin of the curvature of the Southern Andes has also been proposed (Ramos and Aleman, 2000), and was partially validated by lithospheric-scale analogue experiments by Diraison et al. (2000). Whether the Late Cretaceous orogeny involved oroclinal rotation or not is hard to discern from present paleomagnetic data (Rapalini et al., in press), but it clearly produced the consolidation of the basement domain by latest Cretaceous time (Cunningham, 1995; Kraemer, 2003). Afterwards, the basement formed a curved rigid indenter that produced the compressional pattern observed in the Magallanes fold-and-thrust belt, as shown by sand-box models (Ghiglione and Cristallini, 2007). Latest models proposed a two-stage evolution of the curvature of the Southern Andes consisting of a Late Cretaceous phase of oroclinal bending during closure of the Rocas Verdes basin, followed by formation of the primary curvature of the Magallanes fold-and-thrust belt during the Cenozoic (Poblete et al., 2014).

The poorly constrained kinematic evolution of the Southern Andes is also reflected into the debated origin of the Cordillera Darwin metamorphic complex (hereafter referred to as 'Cordillera Darwin') exposed near the hinge of the curvature at ~55°S (Fig. 2). Although several Paleozoic to Mesozoic metamorphic complexes are exposed in the Patagonian Andes to the north (Hervé et al., 2008), the processes for the exhumation of Cordillera Darwin remains the most debated (Cunningham, 1995; Dalziel and Brown, 1989; Klepeis, 1994; Kohn et al., 1995; Maloney et al., 2011). Cordillera Darwin exposes Paleozoic basement rocks metamorphosed under upper amphibolite to greenschist facies conditions (7-11 kbar, 580-600 °C) (Klepeis et al., 2010; Kohn et al., 1993, 1995; Nelson et al., 1980). Kohn et al. (1995) proposed an initial rapid exhumation at 90-70 Ma driven by extension (or transtension), while more external sectors were under compression. Similarly, Dalziel and Brown (1989) argued that the exhumation began at ca. 70 Ma in a localized extensional setting within a developing transform zone between the South American and Antarctic plates. On the other hand, several models were proposed by Cunningham (1995) who related the exhumation to (i) erosional denudation within a restraining bend setting, (ii) transtension, or (iii) erosion and/or extension following isostatic rebound. The most broadly accepted model for the uplift of Cordillera Darwin considers thick-skinned compressional tectonics coupled with widespread erosion (Barbeau et al., 2009; Gombosi et al., 2009; Klepeis, 1994; Klepeis and Austin, 1997; Klepeis et al., 2010; Maloney et al., 2011; Torres Carbonell and Dimieri, 2013).

Understanding the tectonic regime at the Southern Andes during the Late Cretaceous and Paleogene is therefore key to untangle the evolution of the Patagonian Orocline and the exhumation history of Cordillera Darwin. In this study, we reconstruct the nature and orientation of the strain field at the Southern Andes from the Cretaceous throughout the Oligocene using both new and published anisotropy of magnetic susceptibility (AMS) data from the Magallanes fold-and-thrust belt.

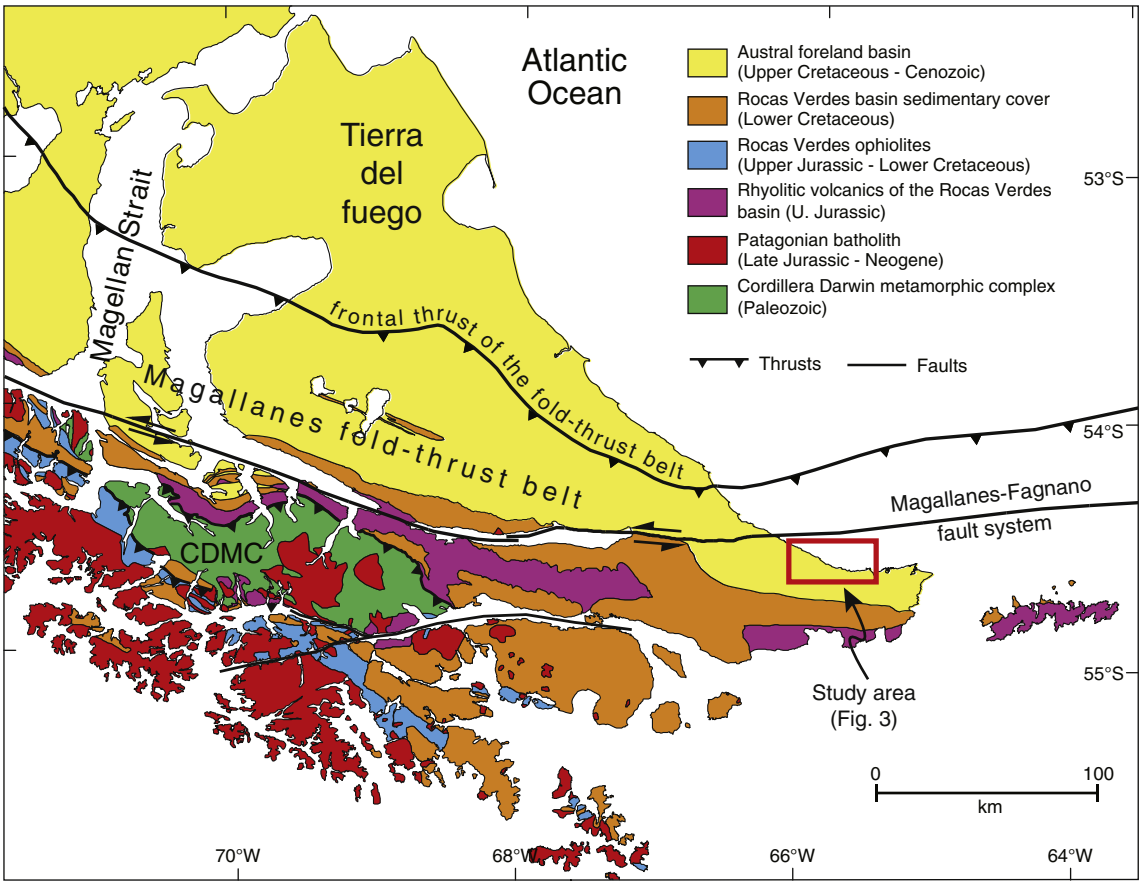

Fig. 2. Regional geological map of the Fuegian Andes showing the main tectono-stratigraphic domains, and the sampling area.

2. Background

2.1. Geological Setting

Four tectonic provinces can be recognized in the Southern Andes (Fig. 2), from SW to NE: (i) a coastal magmatic arc, including the calc-alkaline igneous suite from the Patagonian Batholith emplaced between the Late Jurassic and Neogene (González-Guillot et al., 2011; Hervé et al., 1984, 2007; Pankhurst et al., 2000); (ii) the Rocas Verdes marginal basin units, including weakly metamorphosed relics of its ocean floor (Sarmiento and Tortuga ophiolite complexes; Stern and De Witt, 2004; Cunningham, 1994) and its sedimentary cover (Calderón et al., 2007; Olivero and Malumián, 2008); (iii) Cordillera Darwin exposing late Paleozoic basement schists affected by thick-skinned tectonics (Hervé et al., 2008; Klepeis, 1994; Klepeis et al., 2010; Kohn et al., 1995; Maloney et al., 2011, 2013); and (iv) the thin-skinned Magallanes fold-and-thrust belt, developed within a ~7 km thick (Austral) foreland basin containing Upper Cretaceous to Miocene marine sequences (Alvarez-Marron et al., 1993; Biddle et al., 1986; Ghiglione and Ramos, 2005; Ghiglione et al., 2002; Klepeis, 1994; Malumián and Olivero, 2006; Olivero and Malumián, 1999, 2008; Olivero and Martinioni, 2001; Olivero et al., 2003; Torres Carbonell et al., 2008).

The Magallanes fold-and-thrust belt is composed of ~ E-verging (Patagonian Andes) and ~ N-verging (Fuegian Andes) thrust sheets that involve progressively younger units towards the foreland (Fig. 2): Upper Jurassic-Lower Cretaceous formations in the inner domain, and Upper Cretaceous to Neogene in the most external sectors (Ghiglione and Ramos, 2005; Menichetti et al., 2008; Olivero and Malumián, 1999, 2008; Olivero and Martinioni, 2001). The Neogene left-lateral Magallanes–Fagnano Fault Zone cuts the northern domain of the fold-thrust belt (Lodolo et al., 2003) forming a transtensional pull-apart basin along the Irigoyen River (Ghiglione, 2003). This fault system, crossing the entire island of Tierra del Fuego, is considered the onshore segment of the South America–Scotia plate boundary, along which prominent asymmetric pull-apart basins developed (Lodolo et al., 2002, 2003).

2.2. Tectonic history of the Southern Andes

The Middle-Late Jurassic evolution of the Southern Andes included widespread silicic subaerial volcanism along the present Pacific continental margin coevally with the breakup of Antarctica from South America (Bruhn et al., 1978; Calderón et al., 2007; Pankhurst et al., 2000). Prolonged extension along the South American margin culminated in the Late Jurassic opening of the Rocas Verdes marginal basin (Bruhn and Dalziel, 1977; Bruhn et al., 1978; Calderón et al., 2007; Dalziel, 1981; Dalziel et al., 1974; Katz, 1973). The extensional phase also affected more internal sectors of the South American continent, yielding widespread normal faults and crustal attenuation that are thought to have played a key role during later foreland propagation of the deformation (Fosdick et al., 2011, 2014; Likerman et al., 2013; Winslow, 1982). The first sedimentary infill of the marginal basin is represented by the Upper Jurassic to Lower Cretaceous submarine silicic volcanics and volcaniclastic levels of the Tobifera (or Lemaire) formation, and dark mudstones of the Yahgan (or Zapata) formation, followed by slope mudstones of the Beauvoir Formation (Fildani and Hessler, 2005; Klepeis et al., 2010; Menichetti et al., 2008; Olivero and Malumián, 2008; Wilson, 1991). In the Early Cretaceous, the opening of the South Atlantic Ocean associated with increased subduction rates along the Pacific margin (Dalziel, 1986; Diraison et al., 2000; Rabinowitz and LaBrecque, 1979; Ramos, 1989; Somoza and Zaffarana, 2008) induced sinistral transpression along the southwestern margin

of South America (Cunningham et al., 1995; Klepeis, 1994). This event caused tectonic inversion (i.e., extension to compression) in the retro-arc region that was accommodated by trench-ward underthrusting of the South American craton down to ~35 km depth (Bruhn, 1979; Cunningham, 1995; Klepeis et al., 2010; Wilson, 1991). Ductile deformation, isoclinal folding and low-grade metamorphism in the marginal basin sedimentary units (Bruhn, 1979), and peak metamorphism at upper amphibolite facies conditions (7-11 kbar and 580–600 °C; Kohn et al., 1993) in the underthrust basement rocks currently exposed in Cordillera Darwin (Klepeis et al., 2010; Maloney et al., 2011) marked the onset of the earliest tectonic phase in the Southern Andes.

Complete closure of the Rocas Verdes marginal basin and collision between the magmatic arc and the South American continental margin was achieved in the Late Cretaceous (Bruhn and Dalziel, 1977; Calderón et al., 2012; Cunningham, 1994, 1995; Halpern and Rex, 1972), and produced initial uplift of continental basement blocks. This included Cordillera Darwin whose uplift and exhumation has been initially constrained by $^{40}Ar/^{39}Ar$ and fission–track thermochronology showing two major pulses at 90-70 Ma and 60-40 Ma (Kohn et al., 1995; Nelson, 1982). U/Pb detrital-zircon geochronology from the eastern Magallanes foreland basin documented a dramatic provenance shift at ca. 39 Ma, suggesting that the metamorphic Paleozoic basement was completely exposed by that time (Barbeau et al., 2009). Apatite and zircon fission-track and (U-Th-Sm)/He data (Gombosi et al., 2009) indicate, consistently with the conclusions of Barbeau et al. (2009), a rapid exhumation that occurred in the middle-late Eocene (40-35 Ma), followed by slower exhumation rates. Early contraction events in the basement domains have been recently constrained at ca. 85-86 Ma in the Fuegian Andes (Klepeis et al., 2010), and ca. 85 Ma in the Southern Patagonian Andes (Calderón et al., 2012).

Progressive crustal thickening in the inner sectors of the Southern Andes, characterized by out-of-sequence thrusting, continued throughout the Late Cretaceous and Paleogene, yielding lithospheric loading and flexural subsidence in the Magallanes (or 'Austral') and Malvinas foreland basins (Alvarez-Marron et al., 1993; Biddle et al., 1986; Coutand et al., 1999; Fildani et al., 2003; Ghiglione et al., 2010; Klepeis, 1994; Ramos, 1989; Wilson, 1991; Winslow, 1981). Major and minor unconformities within the foreland basin in the Fuegian Andes have been associated with a number of tectonic pulses, including the late Paleocene San Vicente thrusting episode (61-55 Ma), the Eocene Rio Bueno thrusting event (49-34 Ma), and other minor events in the early Eocene and late Oligocene (Alvarez-Marrón et al., 1993; Ghiglione and Ramos, 2005; Olivero and Malumián, 2008; Olivero et al., 2003; Torres Carbonell and Dimieri, 2013; Torres Carbonell et al., 2008, 2011, 2013). Uncertainties still exist on the age of the earliest tectonic pulses in the foreland basin of the Fuegian Andes, and older (i.e., pre-62 Ma) events have also been proposed (Torres Carbonell et al., 2013). The Punta Gruesa strike-slip event (ca. 24-16 Ma) defines the initial tectonic phase associated to the development of the Magallanes-Fagnano Fault Zone and the active strike-slip deformation (Cunningham, 1993, 1995; Eagles et al., 2005; Lodolo et al., 2003; Rossello, 2005). Then, subhorizontal units above lower Miocene beds mark the end of compressional tectonics in the southern Magallanes basin (Ghiglione, 2002; Ghiglione et al., 2010).

There are insufficient age constraints along strike (in space and time) to test whether the tectonic phases were synchronous throughout the Southern Andes. The available data, however, indicate that at least some events were coeval both in the Patagonian and Fuegian Andes. During the Paleocene, deformation in the Patagonian Andes was mainly localized in the basement domain (Kraemer, 1998). Subsequent collision of the Farallon-Phoenix ridge in the middle Eocene (Cande and Leslie, 1986; Somoza and Ghidella, 2005, 2012) produced reactivation and eastward shifting of the orogenic front. This event produced angular unconformities and growth-strata at Río Turbio (Malumián et al., 2000), and emplacement of an Eocene basaltic plateau (*Mesetas*) (Ramos, 1989, 2005). A major thrusting event and uplift in the Paleogene has been also constrained using zircon (U-Th)/He dating from the eastern domains of the southern Patagonian Andes (Fosdick et al., 2013). The Eocene tectonics became much stronger towards the south affecting in particular Tierra del Fuego due to fast ~ NE-directed subduction of the Phoenix plate between 47-28 Ma (Ghiglione and Cristallini, 2007; Ghiglione and Ramos, 2005; Kraemer, 2003; Olivero and Martinioni, 2001; Ramos and Aleman, 2000; Somoza and Ghidella, 2005, 2012). Apatite fission track, and apatite and zircon (U-Th)/He ages constrained compressive events in the western domains of the Patagonian Andes to the late Oligocene (30-23 Ma; Thomson et al., 2001), which then propagated to the east during the early Miocene (22-18 Ma; Fosdick et al. (2013) and middle to late Miocene (12-8 Ma; Thomson et al., 2001).

The space-time evolution and magnitude of the strike-slip tectonics at the Southern Andes is even more difficult to constrain. While it is commonly accepted that sinistral strike-slip faulting, mainly associated with the South America-Antarctica relative plate motion, affected the Fuegian Andes in the late Cenozoic (Ghiglione and Ramos, 2005; Lodolo et al., 2003; Menichetti et al., 2008; Rossello, 2005), the origin of dextral Miocene (16-10 Ma) strike- faults in the southern Patagonian Andes is less certain, and possibly associated to the Phoenix-Antarctica ridge subduction event (Thomson, 2002).

3. Anisotropy of magnetic susceptibility (AMS): methodology

Anisotropy of magnetic susceptibility (AMS) is a petrofabric tool able to determine the preferred orientation of magnetically-dominant minerals, and it is commonly used as a rock strain indicator (e.g., Jelinek, 1977, 1978; Hrouda, 1982, 1993; Borradaile, 1988, 1991; Jackson, 1991; Jackson and Tauxe, 1991; Rochette et al., 1992; Tarling and Hrouda, 1993; Sagnotti et al., 1994, 1998; Parés et al., 1999; Soto et al., 2009). In weakly deformed sedimentary rocks, AMS reflects the initial fabric produced during incipient deformation (mainly related to layer-parallel shortening) at the time of, or shortly after, deposition and diagenesis of the sediment (Sintubin, 1994; Sagnotti et al., 1998, 1999; Parés et al., 1999; Cifelli et al., 2004, 2005; Larrasoaña et al., 2004; Soto et al., 2009). For this reason AMS analyses of weakly deformed sediments have frequently been used in orogenic settings to document the syn-sedimentary tectonic regime (Mattei et al., 1999; Sagnotti and Speranza, 1993; Sagnotti et al., 1998; Parés et al., 1999; van Hinsbergen et al., 2005; Maffione et al., 2012; Gong et al., 2009; Macrì et al., 2014, among many others).

AMS can be geometrically described by an ellipsoid, whose axes are the minimum (k_{min}), intermediate (k_{int}), and maximum (k_{max}) axis of susceptibility (Hrouda, 1982). During deposition, sedimentary rocks acquire a so-called 'sedimentary fabric' characterized by the k_{max} and k_{int} axes dispersed within a plane (magnetic foliation, F) that is subparallel to the stratification plane. A sedimentary fabric can be partially overprinted by a 'tectonic fabric' during incipient deformation (e.g., Parés et al., 1999). The result of this process is the development of a magnetic lineation (L) whereby k_{max} axes align parallel to the maximum axis of stretching (ε_1). For weak strain, the AMS ellipsoid is congruent to the orientation of the strain ellipsoids (e.g., Parés et al., 1999).

In extensional settings, the magnetic lineation has been found to be parallel to the stretching direction and local bedding dip, and hence perpendicular to local normal faults (Cifelli et al., 2004, 2005; Maffione et al., 2012; Mattei et al., 1997, 1999; Sagnotti et al., 1994). In compressive settings, the magnetic lineation is usually sub-horizontal and parallel to both the local strike of the strata and folds axes (e.g., Mattei et al., 1997; Sagnotti and Speranza, 1993; Sagnotti et al., 1998). The relationship between the direction of the magnetic lineation and the local attitude of the studied rock is therefore often diagnostic to discriminate the tectonic regime (compressive versus extensional) responsible for the origin of the magnetic lineation (Mattei et al., 1997).

Increasing strain progressively modifies the shape of the AMS ellipsoid from a pure sedimentary fabric (oblate ellipsoid: $k_{max} \approx k_{int} >> k_{min}$), to a sedimentary fabric with a marked tectonic overprint (triaxial ellipsoid: $k_{max} > k_{int} > k_{min}$), to a pure tectonic fabric

(prolate ellipsoid: $k_{max} > > k_{int} \approx k_{min}$), and eventually returning to an oblate ellipsoid with the magnetic foliation parallel to the cleavage/schistosity (Parés, 2004). Such a progression has previously been identified in the Southern Pyrenean foreland basin (Parés et al., 1999). In the last stage of deformation, which corresponds to incipient metamorphism, the tectonic fabric developed during the initial (syn-sedimentary) phases of deformation is overprinted and lost, whereas it is preserved under small strains at low temperature (e.g., Larrasoaña et al., 2004; Parés, 2004; Soto et al., 2009). This implies that the finite strain inferred from AMS analyses of weakly deformed rocks can provide, in combination with structural geological analysis, fundamental constraints to study the tectonic regime (style and orientation) accompanying the deformation of sedimentary basins.

4. Sampling and methods

Samples were collected from Upper Cretaceous to upper Eocene sedimentary rocks from the most internal domains of the Magallanes fold-and-thrust belt (south of the Magallanes-Fagnano Fault Zone) along the Atlantic coast of Peninsula Mitre (Fig. 2). The sampled rocks are folded and faulted, but without any evidence of metamorphism or pervasive cleavage. A total of 286 cores were collected at 22 sites from six different formations (Fig. 3, Table 1). Four sites were collected from the Maastrichtian-Danian Policarpo Formation (>700 m-thick) represented by highly bioturbated dark slaty mudstones and sandstones deposited in the earliest, innermost Bahía Tethis foreland depocenter (Olivero and Malumián, 1999; Olivero and Martinioni, 2001). This formation is overthrust in the south by the pervasively cleaved upper Campanian-lower Maastrichtian Bahia Tethis Formation and, at the sampling locality, it is unconformably covered by the Rio Bueno Formation. Eight sites were drilled in the upper Paleocene La Barca Formation (220 m-thick), composed of tuffaceous sandstones, siltstones and black mudstones. Three sites were sampled in the upper Paleocene-lower Eocene Punta Noguera Formation (380 m-thick), consisting of glauconitic gravity flows deposits, including massive tuffaceous sandstones and sandy turbidites. One site was drilled in the lower Eocene Cerro Ruperto Formation (200 m-thick), glauconite-rich, silty sandstones and siltstones (Olivero and Malumián, 1999). One site was drilled in the lower-middle Eocene rhythmically bedded grainstones of the Río Bueno Formation (~80 m-thick). Five sites were sampled within the middle-upper Eocene dark gray mudstones of the Cerro Colorado Formation (855 m-thick).

Samples were collected in the field with a petrol-powered portable drill cooled by water, and oriented with a magnetic compass, which was corrected for the local magnetic declination (11° E at the time of sampling, December 2012). All the laboratory analyses were conducted at the paleomagnetic laboratory of the Istituto Nazionale di Geofisica e Vulcanologia (Rome, Italy). Low-field AMS was measured with Multi-Function Kappabridge (MFK1-FA, AGICO). The AMS parameters at both the specimen and the site levels were evaluated according to Jelinek statistics (1977, 1978) using the Anisoft 4.2 software (AGICO). Rock magnetic experiments on representative samples were also performed to investigate the main mineral fraction responsible for the AMS. Natural remanent magnetization (NRM) was measured from all samples using a 2G Enterprise DC-SQUID superconducting cryogenic magnetometer. Thermal variation (20-700 °C) of magnetic susceptibility was measured at four representative samples from site CJ04, CR01, RL01, and RL03 with an MFK1-FA Kappabridge (AGICO) coupled with a CS-3 device. Hysteresis cycles were performed with a Micromag AGM (maximum applied field 1 T) on the same samples used for the thermomagnetic curves.

5. Results

A well-defined magnetic fabric has been identified at 21 out of 22 sites, with site RL02 showing an isotropic fabric (Fig. 4 and Table 1). Site mean susceptibility (k_m) in the studied samples varies between 1.24 and 4.13 x 10^{-4} SI (with more frequent values in the range 1.2-3.2 x 10^{-4} SI) (Fig. 5a; Table 1). NRM is generally low and ranges between 0.16 and 2.01 mA/m (Table 1). Both thermomagnetic curves and hysteresis cycles indicate the predominance of paramagnetic minerals on the low-field magnetic susceptibility (Fig. 5b,c). This evidence indicates that the AMS is mainly controlled by a phyllosilicate paramagnetic matrix (e.g., Borradaile et al., 1987; Hrouda and Jelinek, 1990; Rochette, 1987).

Site mean anisotropy degree (P') values are commonly low ($P' < 1.120$), with 20 sites showing P' values lower than 1.070 (Fig. 5d; Table 1). Fig. 5d shows that, within each unit, k_m and P' are not correlated, implying that the variation of P' may be proportional to the strain rather than to the concentration and nature of the ferromagnetic fraction. We note, however, that for site RL01 a high P' value correspond to an equally high susceptibility (Table 1); the anisotropy degree in this case might be controlled by the mineralogy rather than the strain.

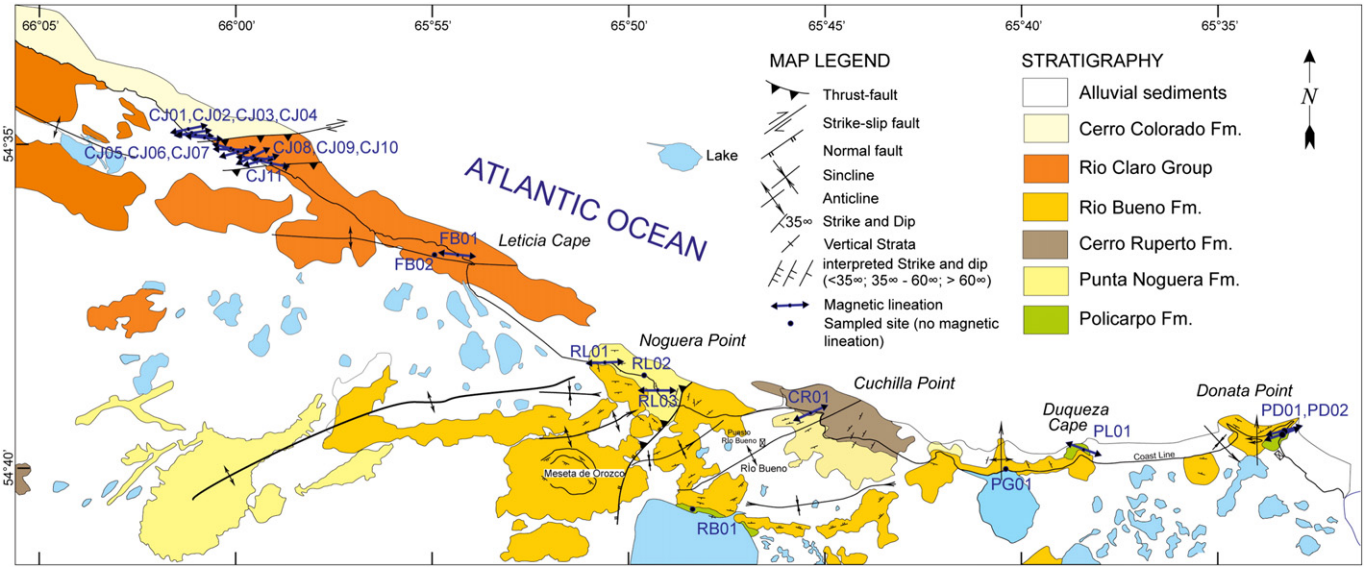

Fig. 3. Geological map of the study area showing the sampled sites and the directions of the site mean magnetic lineation (blue arrows).

Table 1
Anisotropy of magnetic susceptibility (AMS) results from the internal domains of the Magallanes fold-and-thrust belt.

Site	Formation	Lat (S)	Long (W)	Age	Bedding	N	NRM	k_m	L	F	P'	T	D (°)	I (°)	e_{12} (°)	AMS origin
RB01	Policarpo	54° 40' 30.66"	65° 48' 39.13"	Maastr. – Danian	182/74	9	0.28	1.33	1.002	1.004	1.007	0.256	189.9	34.8	34.2	T ?
PD01	Policarpo	54° 38' 57.77"	65° 33' 15.85"	Maastr. – Danian	347/55	25	1.20	2.19	1.008	1.004	1.012	-0.320	255.9	23	22.9	T, c
PD02	Policarpo	54° 39' 3.83"	65° 33' 24.51"	Maastr. – Danian	330/55	10	0.39	1.53	1.012	1.012	1.024	-0.005	250.4	27.1	13.4	T, c
PL01	Policarpo	54° 39' 30.58"	65° 38' 30.23"	Maastr. – Danian	158/45	16	0.21	1.24	1.009	1.007	1.016	-0.130	290.5	9.1	12.6	T, ?
CJ05	La Barca	54° 35' 25.24"	66° 00' 43.60"	L. Paleocene	267/35	12	1.01	1.84	1.008	1.028	1.038	0.575	284.5	27.6	26.0	T, c
CJ06	La Barca	54° 35' 26.72"	66° 00' 41.57"	L. Paleocene	260/33	9	0.97	1.89	1.009	1.033	1.045	0.550	272.3	17.0	9.2	T, c
CJ07	La Barca	54° 35' 27.43"	66° 00' 38.49"	L. Paleocene	266/34	11	0.72	1.77	1.010	1.026	1.037	0.456	255.2	18.8	12.0	T, c
CJ08	La Barca	54° 35' 28.16"	66° 00' 35.47"	L. Paleocene	308/34	8	0.60	1.60	1.007	1.018	1.025	0.443	243.9	19.9	40.8	T, c
CJ09	La Barca	54° 35' 30.87"	66° 00' 21.37"	L. Paleocene	202/51	8	2.01	1.93	1.021	1.037	1.060	0.273	274.6	12.3	13.5	T, c
CJ10	La Barca	54° 35' 34.58"	66° 00' 03.13"	L. Paleocene	182/53	8	1.17	1.85	1.028	1.031	1.060	0.044	251.1	16.0	8.1	T, c
FB01	La Barca	54° 36' 38.78"	65° 54' 54.16"	L. Paleocene	022/57	10	0.18	1.27	1.010	1.016	1.026	0.213	99.2	21.1	21.0	T, c
FB02	La Barca	54° 36' 35.37"	65° 56' 43.11"	L. Paleocene	162/77	9	0.23	1.93	1.001	1.014	1.017	0.806	236.6	18.2	72.0	S
RL01	Punta Noguera	54° 38' 23.98"	65° 50' 59.09"	L. Paleoc. - E. Eoc.	192/31	9	1.71	4.13	1.092	1.032	1.131	-0.472	264.8	11.8	22.3	T, c
RL02	Punta Noguera	54° 38' 36.38"	65° 49' 40.01"	L. Paleoc. - E. Eoc.	192/31	8	1.36	3.05	-	-	-	-	-	-	-	-
RL03	Punta Noguera	54° 38' 47.49"	65° 49' 32.20"	L. Paleoc. - E. Eoc.	192/31	7	1.28	2.63	1.023	1.081	1.112	0.544	269.5	27.5	30.6	T, c
CR01	Cerro Ruperto	54° 39' 06.19"	65° 45' 14.84"	E. Eocene	347/34	22	1.84	3.00	1.037	1.005	1.046	-0.775	65.3	6.8	17.6	T, c
PG01	Rio Bueno	54° 39' 43.59"	65° 40' 19.30"	M. Eocene	084/4	24	0.32	1.48	1.007	1.053	1.067	0.753	150.0	7.1	30.3	S
CJ01	Cerro Colorado	54° 35' 11.59"	66° 01' 46.03"	M. – L. Eocene	354/37	19	0.22	2.48	1.016	1.012	1.028	-0.139	257.9	12.5	24.5	T, c
CJ02	Cerro Colorado	54° 35' 13.82"	66° 01' 41.81"	M. – L. Eocene	002/23	12	0.21	2.60	1.011	1.031	1.044	0.456	83.1	1.7	14.1	T, c
CJ03	Cerro Colorado	54° 35' 15.31"	66° 01' 35.39"	M. – L. Eocene	356/31	10	0.16	2.50	1.010	1.021	1.032	0.334	273.5	2.4	13.7	T, c
CJ04	Cerro Colorado	54° 35' 17.27"	66° 01' 25.96"	M. – L. Eocene	350/39	24	0.27	2.36	1.012	1.021	1.033	0.282	276.4	0.7	26.9	T, c
CJ11	Cerro Colorado	54° 35' 37.89"	65° 59' 44.66"	M. – L. Eocene	357/38	16	0.43	2.68	1.018	1.046	1.067	0.423	282.2	1.1	19.2	T, c

Geographic coordinates use WGS84 datum. Bedding is expressed as dip direction/dip. N, number of studied samples at a site. NRM, natural remanent magnetization expressed in 10^{-3} A/m. k_m, site mean susceptibility in 10^{-4} SI. Magnetic lineation (L), magnetic foliation (F), corrected anisotropy degree (P'), and shape factor (T) according to Jelinek (1978). D and I are the *in-situ* site-mean declination and inclination, respectively, of the maximum susceptibility axis. e_{12}, semi-angle of the 95% confidence ellipse around the declination of the mean lineation. 'AMS origin' indicates the interpreted nature of the AMS (T = tectonic, S = sedimentary), and related tectonic style (c = compressive).

A change in the shape of the AMS ellipsoid, from strongly oblate ($T \approx 1$, $F >> L$), to triaxial ($T \approx 0$, $F \approx L$), to strongly prolate ($T \approx -1$, $L >> F$) is observed within the sampled sites, with no apparent spatial pattern (Fig. 5e; Table 1). Such variation describes a path that matches (when site RL01 is excluded) the expected evolution of the AMS ellipsoid during increasing strain (Borradaile and Henry, 1997; Parés et al., 1999).

A pure sedimentary fabric is observed at sites FB02 and PG01, where the AMS ellipsoid is strongly oblate ($F >> L$), and the k_{int} and k_{max} susceptibility axes are not clearly resolved (Figs. 4 and 5e; Table 1). Site RB01 displays a triaxial AMS ellipsoid, yet it has a very low degree of anisotropy (P' = 1.007; Table 1) that makes the tectonic origin for its magnetic fabric arguable. Therefore, these three sites will not be considered for following tectonic reconstructions.

The magnetic fabric of the remaining 18 sites indicates a tectonic overprint of the original sedimentary fabric. Within this group, the AMS ellipsoids of 12 sites are mainly oblate ($T > 0$), with a strong triaxial tendency (i.e., the three susceptibility axes form distinct clusters) and the magnetic foliation plane sub-parallel to the strata (the pole to local bedding is comprised within the distribution of the k_{min} axes; see Fig. 4 and Table 1). These are all typical features of weakly deformed rocks (e.g., Borradaile, 1987; Borradaile and Jackson, 2004). A mainly prolate fabric ($T < 0$), showing a girdle distribution of the k_{int} and k_{min} axes perpendicular to the k_{max} mean orientation dominates at six sites (three from the Policarpo Formation; Table 1 and Fig. 4). One of these sites (CR01) shows a magnetic fabric resembling that of typical pencil structure, a stage that predates the development of a macroscopic cleavage upon moderate to high deformation (e.g., Borradaile and Tarling, 1981). Although cleavage was not recognized in the sampled rocks, it is likely that the six sites characterized by a prolate AMS ellipsoid were affected by a higher strain.

Magnetic lineation is well developed ($e_{12} < 30°$; Table 1) at 16 out of the 18 sites characterized by tectonic overprint. Two remaining sites show a moderately-developed, yet still defined, magnetic lineation ($30° < e_{12} < 40.8°$; Table 1). The mean magnetic lineation is subhorizontal or shallowly plunging and parallel to both the local strike of the unit and nearby fold axes at 14 sites, subparallel to the dip direction of the strata at two sites (CJ05-07), and oblique to the local strike of the bedding at site PL01 (Figs. 3 and 4). All sites but RB01 show a mean lineation trending ~ E-W (Fig. 3).

6. Discussion

AMS analyses from the Upper Cretaceous to upper Eocene sedimentary rocks of the internal structural domains of the Magallanes fold-and-thrust belt in Tierra del Fuego revealed a magnetic fabric of tectonic origin at 18 sites (Table 1 and Fig. 3). The shape of the AMS ellipsoids (T) and the anisotropy degree (P') at these sites, combined with the absence of a macroscopic cleavage, indicate that these rocks experienced a low degree of deformation; the initial AMS fabric acquired during (or shortly after) sedimentation is, therefore, likely preserved in these rocks. Similar AMS parameters and lithological features were observed in Cretaceous-Oligocene sedimentary units from the southern and western Magallanes fold-and-thrust belt (Diraison, 1998; Maffione et al., 2010; Poblete et al., 2014). This implies that the magnetic fabric of the foreland basin formations from the Southern Andes very likely preserve a record of the syn-sedimentary tectonics. This allows us to reconstruct the sequence of tectonic events (i.e., their nature and kinematics) that affected the Southern Andes in the Late Cretaceous and Cenozoic.

The shape of the AMS ellipsoid is indicative of the intensity of deformation affecting these rocks (e.g., Parés et al., 1999). Considering the existing AMS database from the Southern Andes (Diraison, 1998; Maffione et al., 2010; Poblete et al., 2014), we infer that the most internal structural domains of the fold-and-thrust belt, exposing Upper Cretaceous to Paleocene rocks, show a predominantly prolate AMS ellipsoid indicative of moderate-to-high strain. Conversely, the oblate-to-triaxial AMS ellipsoids characterizing the younger post-Paleocene formations exposed within the most external domains of the belt are suggestive of relatively weak strain.

6.1. Late Cretaceous-late Eocene tectonic regime in the Magallanes fold-and-thrust belt

Magnetic lineation has frequently been used to infer the nature (extensional vs. contractional) and orientation of the strain field, and draw conclusions on the local tectonic regime (e.g., Gong et al., 2009;

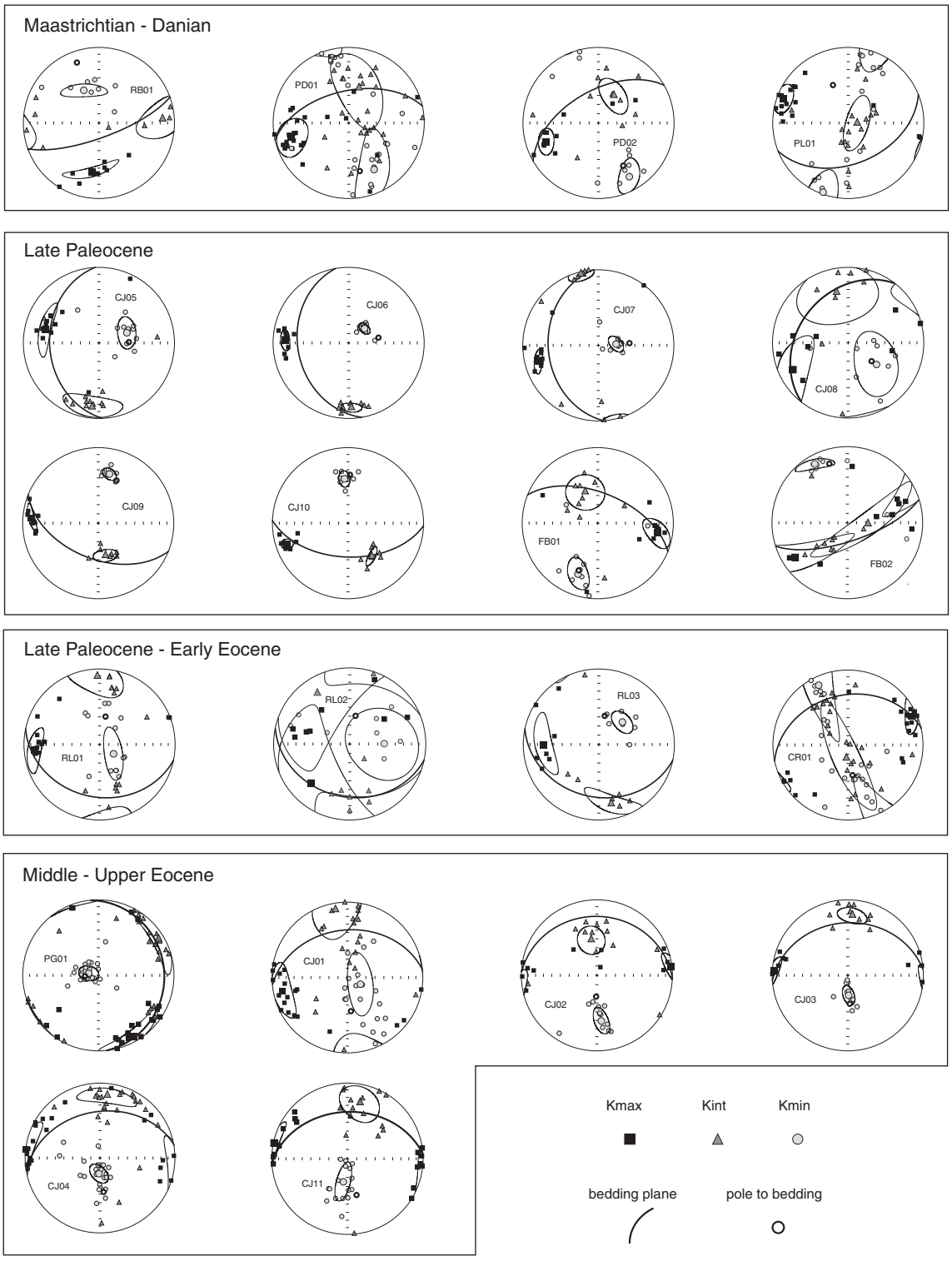

Fig. 4. Schmidt equal-area projections, lower hemisphere, of the (in-situ coordinates) principal axes (k_{max}, k_{int}, and k_{min}) of the AMS ellipsoid from all sampled sites. Mean values of the three susceptibility axes (larger symbols) and relative 95% confidence ellipses are shown for each diagram. Measured bedding plane and relative pole are also shown. All sites are subdivided into four main age groups.

Larrasoaña et al., 2004; Mattei et al., 1997; Soto et al., 2009). In this study, the magnetic lineations from the oldest (non-metamorphic) units located in the most internal sectors of the Magallanes fold-and-thrust belt have been analysed to constrain the kinematics of the earliest tectonic phases in the Fuegian Andes.

Magnetic lineations at 18 sites within the study area have very likely a tectonic origin (Fig. 3). Although paleocurrents may also produce a relatively well-defined magnetic lineation (e.g., Parés et al., 2007; Rees and Woodall, 1975), such a fabric is commonly easily overprinted during initial stages of deformation. Furthermore, the directions of the magnetic lineation from the sampled sites are slightly different from the regional paleocurrent directions, which are NE- to ENE-directed (Torres Carbonell and Olivero, 2012). The clear tectonic overprint of the studied rocks and the directions of the magnetic lineation,

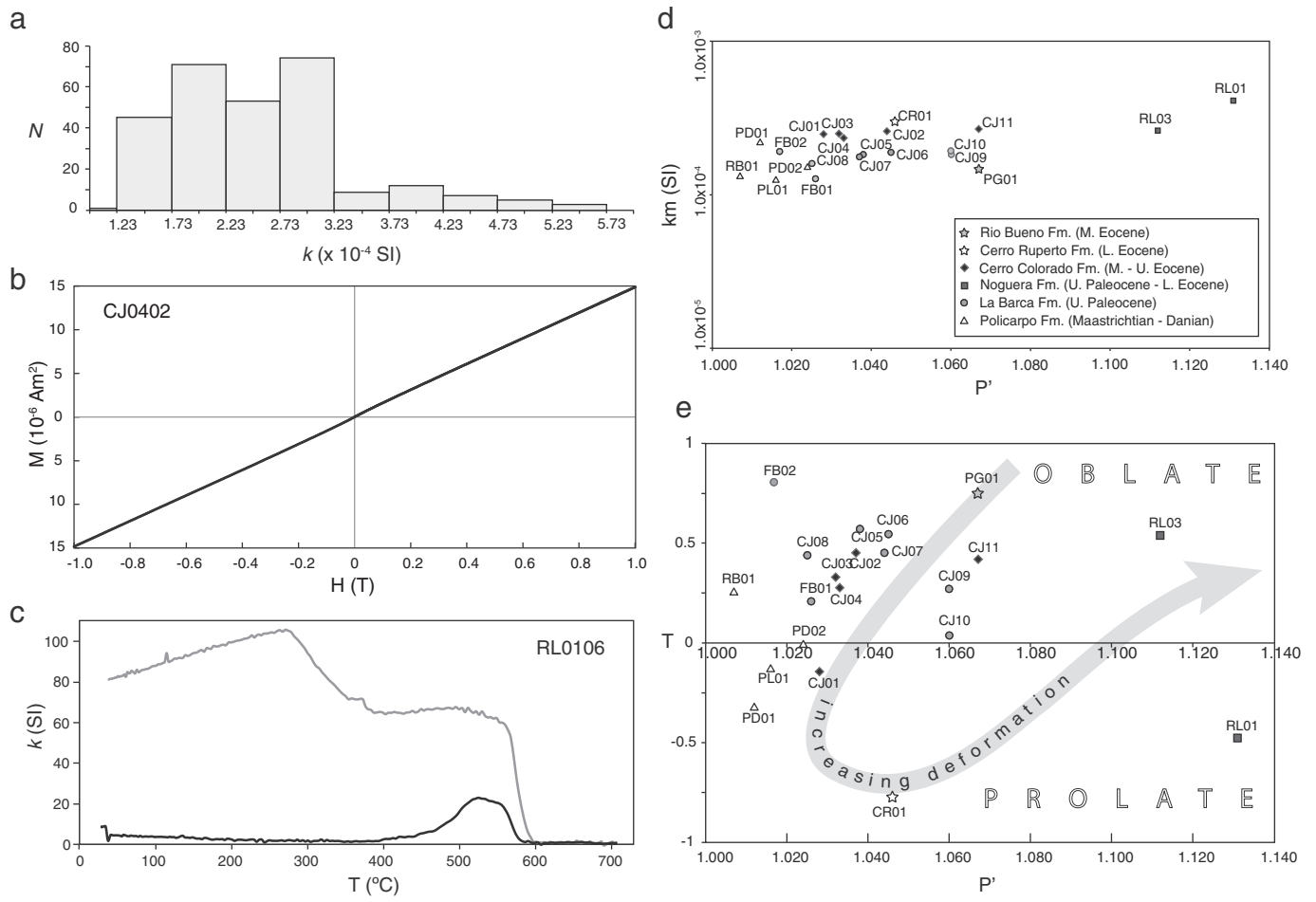

Fig. 5. (a) Frequency distribution of the magnetic susceptibility (k) from all the sampled specimens; (b) site mean susceptibility versus corrected anisotropy degree (P') for all the sampled sites; (c) shape factor (T) versus corrected anisotropy degree (P') diagram compared to the typical trend expected from increasing deformation degrees.

therefore, make paleocurrents an unlikely source of the lineation in the studied rocks.

Sub-horizontal magnetic lineations at 14 sites (Figs. 3 and 4; Table 1) are generally subparallel to both the strike of the strata and local fold axes. Following criteria of Mattei et al. (1997), these relationships indicate a predominantly compressive tectonic setting at the time of sedimentation (or subsequent diagenesis) of each sedimentary unit. The shortening direction is therefore inferred to be perpendicular to the lineation.

Within the remaining four sites, three upper Paleocene sites from the La Barca Formation (CJ05, CJ06, and CJ07) show a magnetic lineation that is sub-parallel to the local dip direction of the strata compatible, *sensu* Mattei et al. (1997) with an extensional tectonic origin of the lineation. The direction of the mean lineations at these three sites is, however, statistically indistinguishable (the confidence ellipses around the mean directions overlap; see Fig. 4) from that of adjacent, coeval sites CJ08, CJ09, and CJ10, which show a clear compressive origin of the lineation. Furthermore, sites CJ05, CJ06, and CJ07 lie along the crest of a ~ E-W trending, westward plunging syncline (Fig. 3). We propose that the magnetic lineations of these sites formed by layer-parallel shortening, within the same tectonic regime that affected nearby sites, and were subsequently tilted to the west subparallel to local hinges during progressive folding.

The remaining site PL01 (Policarpo Formation) shows a horizontal lineation that is not contained in the bedding plane, is at high angle to the strike of the strata, and has a direction that is significantly different from that of adjacent, coeval sites (Fig. 4). Mismatch between the lineation and the bedding attitude might be related to uncertainties in the definition of the bedding plane (stratification of the Policarpo Formation was not well developed) or, more likely, to a high internal strain, as the prolate shape of the AMS ellipsoid seems to suggest. Because of these uncertainties, we cannot unequivocally interpret the nature of the deformation (i.e., extensional versus contractional) affecting this site using the criteria adopted so far; site PL01 is therefore discarded from further analyses.

In summary, a clear compressive origin of the magnetic lineation has been identified at 17 out of the 18 sites showing a tectonic fabric. These sites were subdivided into four age groups, and mean magnetic lineations were calculated for each group (Fig. 6). Sites were distributed as follows: Late Cretaceous-early Paleocene (Policarpo Formation, PD01, PD02), late Paleocene (La Barca Formation, CJ05, CJ06, CJ07, CJ08, CJ09, CJ10, FB01), late Paleocene-early Eocene (Punta Noguera Formation: RL01, RL03; Cerro Ruperto Formation: CR01), middle-late Eocene (Cerro Colorado and Leticia formations, CJ01, CJ02, CJ03, CJ04, CJ11). The four age groups show a consistently ~ E-W-oriented mean magnetic lineation. The orientation of these lineations suggests that the tectonic regime responsible for their origin was relatively stable, yielding continuous ~ N-directed contraction in the internal domains of the Magallanes foreland basin from the Late Cretaceous until the late Eocene (ca. 70 to 35 Ma).

6.2. Strain field at the Southern Andes during the main tectonic phases

A large-scale picture of the tectonic regime active in the Southern Andes during the latest Mesozoic and Cenozoic times has been drawn by using our new and previously published AMS data (Diraison, 1998;

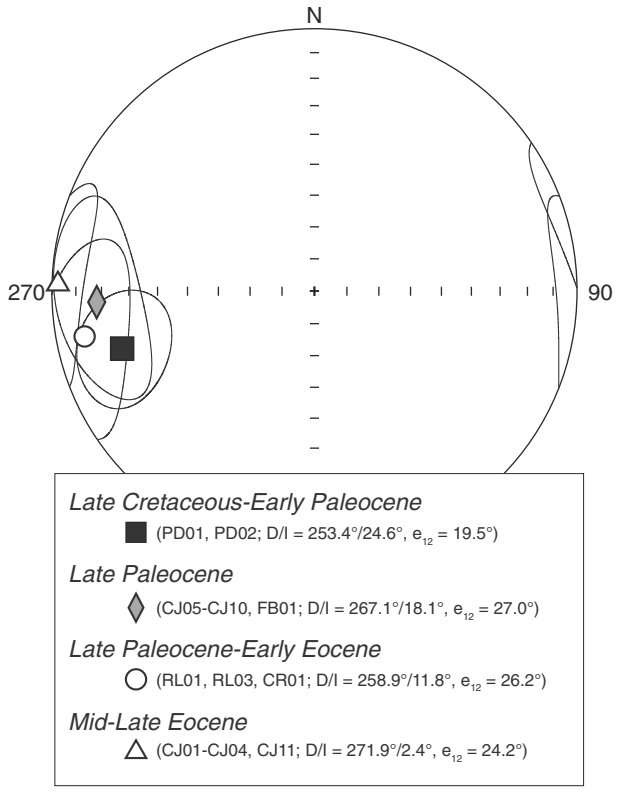

Fig. 6. Schmidt equal-area projections, lower hemisphere, of the mean lineations (k_{max}) and associated 95% confidence ellipses calculated for four age groups. For each group, mean declination (D) and inclination (I) of the lineation, and error associated to the declination (e_{12}) are reported.

Esteban et al., 2011; Maffione et al., 2010; Poblete et al., 2014; Rapalini et al., 2005) and fault kinematics data (Diraison et al., 2000; Torres Carbonell et al., 2013) from this region.

Two AMS studies investigating Jurassic and Cretaceous metamorphic units from the internal sectors of the Fuegian Andes (Esteban et al., 2011; Rapalini et al., 2005) have documented mainly oblate AMS ellipsoids with magnetic foliations coincident with cleavage planes, and magnetic lineations parallel to mineralogical lineations. These features of the magnetic fabric are indicative of a high strain that overprinted the initial fabric acquired during the early stages of deformation. These data, therefore, cannot be considered for the analysis of the syn-sedimentary tectonic events in the Southern Andes. Three more AMS studies have been carried out from non-metamorphic units of the Magallanes fold-and-thrust belt, distributed as follows: sixteen sites from Upper Cretaceous to Cenozoic rocks from both the Patagonian and Fuegian Andes (Diraison, 1998), twenty sites from upper Eocene to lower Miocene formations from the outer part of the fold-and-thrust belt in Tierra del Fuego (Maffione et al., 2010), and 85 sites from Cretaceous to Miocene rocks uniformly distributed throughout the Southern Andes (Poblete et al., 2014). Data reported by these authors (apart from seven sites from Poblete et al. (2014) not used in our analysis because of high internal strain) consistently show oblate to triaxial (and minor prolate) AMS ellipsoids where the magnetic foliations are contained within the bedding planes, and the magnetic lineations are generally sub-horizontal and subparallel to local fold axes, thrust faults, and strikes of the bedding (Fig. 7). The anisotropy degree of these units typically shows low values ($P' < 1.20$ on average). Furthermore the regional paleocurrent directions in the western domain of the Fuegian Andes are ~ NE- to N-oriented (Torres Carbonell and Olivero, 2012), hence almost perpendicular to the magnetic lineations from this area. Relying on this evidence, we conclude that the non-metamorphic units of the Magallanes fold-and-thrust belt have been affected by a weak deformation associated to syn-sedimentary compressive tectonics.

Few attempts of using AMS analyses in strike-slip tectonic settings have been done in the past (e.g., Cifelli et al., 2013; Ferré et al., 2002). Quantifying the effect of such tectonics using AMS constraints, however, may be challenging. Although we cannot exclude, based on AMS data alone, that a transpressive tectonics was active at the time of sedimentation, the parallelism between the magnetic lineation and both the local and regional structural trends suggest that such tectonic style, if active, did not affected the AMS of the studied units.

The selected sites were distributed within four progressive time windows (based on the age of the sedimentary units). For each time window, data were grouped geographically within three main sectors: northern (southern Patagonian Andes), central (western Fuegian Andes), and eastern (eastern Fuegian Andes) (Fig. 7). The mean orientation of the magnetic lineations within the northern sector, where the local faults and fold axes strike 345°, point out to a consistent ENE-WSW-oriented contraction (Fig. 7). In the central sector where faults and fold axes trend 320° to 295°, lineations indicate a mainly NE-SW- to NNE-SSW-oriented shortening (Fig. 7). In the eastern sector near the Atlantic coast, where the regional structural trend varies between 285° and 260°, the mean shortening direction inferred from the lineation data is N-S to NNW-SSE (Fig. 7).

Overall, the magnetic lineations from the Southern Andes mimic the change in direction of the main structural trend of the orogen, describing a radial strain field that is stable over time (Fig. 7). A similar pattern is inferred from the shortening directions obtained from fault kinematic analyses by Diraison et al. (2000). According to these authors, the shortening directions (based on the measurement of 1600 striated fault planes from the Mesozoic-Cenozoic sedimentary cover of the Magallanes fold-and-thrust belt) show a progressive change in orientation from 075° (Patagonian Andes) to 043° (Fuegian Andes). Few data from the easternmost regions of the Fuegian Andes indicate a roughly N-directed shortening, which is also consistent with fault kinematics results obtained from the same area by Torres Carbonell et al. (2013).

Although the geological record from this region is not complete enough to assess whether the main tectonic events have been synchronous across the Patagonian and Fuegian Andes, a partial time overlap of some deformational episodes within the two domains during the Cenozoic (Cande and Leslie, 1986; Thomson et al., 2001; Somoza and Ghidella, 2012; Fosdick et al., 2013) appears to be compatible with our AMS results.

A radial distribution of deformation paths may be a common feature in oroclines or progressive arcs (*sensu* Weil and Sussman, 2004) where the strain trajectories, initially parallel within a rectilinear mountain belt, tend to diverge (or converge) following to subsequent oroclinal bending (e.g., Speranza et al., 1997; Marshak, 2004; Yonkee and Weil, 2010; Weil et al., 2010; Gutiérrez-Alonso et al., 2012; Pastor-Galán et al., 2012; Johnston et al., 2013). Conversely, in primary arcs (*sensu* Weil and Sussman, 2004) where no oroclinal bending is involved, both a uniform and radial strain field can exist (Weil et al., 2010). Key to better interpret our results within a regional tectonic framework is to understand the real nature and origin of the orogenic bend of the Southern Andes.

6.3. The exhumation of the Cordillera Darwin Metamorphic Complex

Although there is growing evidence in support of models requiring compressive tectonics for the exhumation of Cordillera Darwin (Klepeis et al., 2010; Maloney et al., 2011), the tectonic events affecting the Fuegian Andes during the main uplifting phase of Cordillera Darwin have been so far poorly constrained. Relying on structural and geochronological constraints, Klepeis et al. (2010) proposed the occurrence of two early contractional events in the Fuegian Andes. The first tectonic event, likely caused by a flat subduction event (González-Guillot et al., 2011), occurred between 100 and 86 Ma, and caused the inversion of

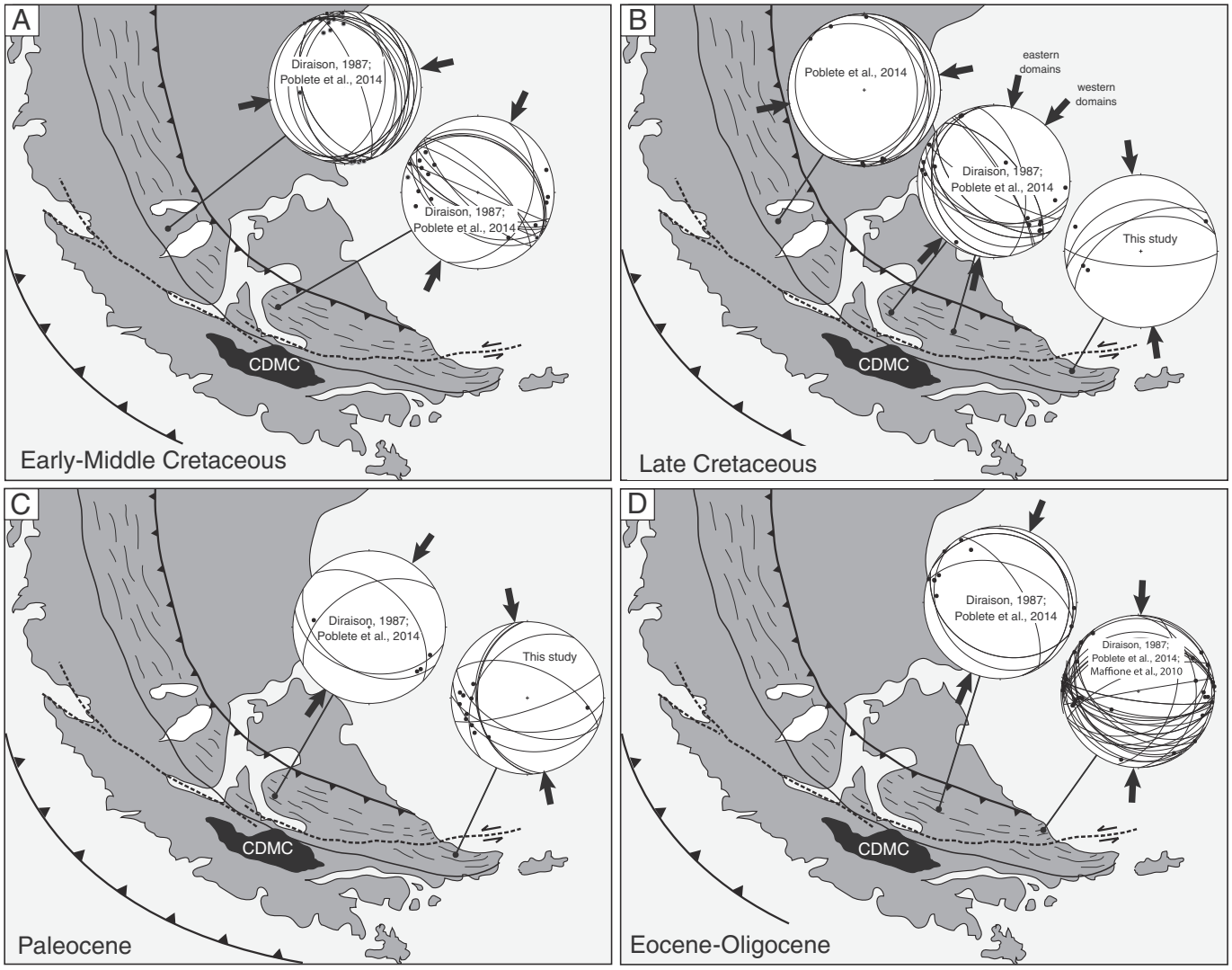

Fig. 7. Four-stage evolution of the paleostrain pattern (black arrows on the stereonets) inferred at the Magallanes fold-thust belt in the Southern Andes based on our new and published AMS data. Stereonets in each sub-figure show the site mean lineations (black dots), and local bedding planes (great circles). CDMC, Cordillera Darwin metamorphic complex.

the Rocas Verdes marginal basin and southward underthrusting of the South American continental margin below the magmatic arc. This age is precisely constrained in Cordillera Darwin by crosscutting relationships between folded sedimentary rocks of the Rocas Verdes basin and Upper Cretaceous granites (86-74 Ma; Kohn et al., 1995). The second tectonic event has been ascribed to a poorly constrained post-80 Ma contractional phase yielding basement-rooted thrust sheet emplacement. Following models of Klepeis et al. (2010), Torres Carbonell and Dimieri (2013) argued that starting from ca. 80 Ma a regional-scale basement duplex system developed along the current axis of the Fuegian Andes above a mid-crustal decoupling surface, yielding uplift in the Fuegian Andes and continuous continent-ward propagation of the compression until the Miocene. It is therefore clear that while the younger (post-middle Paleocene) tectonic phases in the Fuegian Andes are well constrained (e.g., Ghiglione and Ramos, 2005; Torres Carbonell et al., 2013), large uncertainties still exist on the tectonic setting active between ~80 and ~60 Ma, i.e., during initial exhumation phases of Cordillera Darwin.

The AMS results from this study provide new insights on this debated point. Based on the combined database including both our and previous AMS results, we propose that a compressive tectonic regime, yielding shortening perpendicular to the local structural trend of the orogen, was active from at least the Early Cretaceous to the late Oligocene (Fig. 7). We therefore conclude, in agreement with previous models (e.g., Klepeis et al., 2010), that the exhumation of Cordillera Darwin occurred under a general compressive tectonic regime. As suggested by these authors, contraction in the Fuegian Andes yielded a regional-scale crustal duplexing within the Paleozoic basement, which resulted in regional uplift and erosional exhumation of the metamorphic basement currently exposed in Cordillera Darwin.

6.4. An alternative tectonic model for the formation of the Patagonian Orocline

The primary nature of the curvature of the Magallanes fold-and-thrust belt, supported by paleomagnetic data (Maffione et al., 2010; Poblete et al., 2014), requires more complex processes (different from oroclinal bending) to explain the radial strain field documented by this study. Paleomagnetic constraints indicate that the present-day shape of the Southern Andes was likely already acquired in the Late Cretaceous-early Cenozoic before the formation of the Magallanes fold-and-thrust belt. Models considering the indentation of a curved rigid indenter during the Cenozoic (Ghiglione and Cristallini, 2007) to explain the formation of the Magallanes fold-and-thrust belt are, therefore, more consistent with the paleomagnetic evidence. However, the rigid indenter models proposed by Ghiglione and Cristallini (2007)

produced a slightly convergent pattern of deformation paths, much less pronounced than the radial strain field characterizing the Magallanes fold-and-thrust belt.

One plausible mechanism able to reproduce a radial strain field in the foreland basin of the Southern Andes upon indentation of a rigid curved buttress is represented by slip partitioning along pre-existing crustal heterogeneities (e.g., faults). It has been already pointed out the key role of pre-existing Jurassic normal faults rooted in the basement of the South American continental margin in the evolution of the Magallanes foreland basin sedimentation and subsequent deformation (Fosdick et al., 2011, 2014; Ghiglione et al., 2013; Likerman et al., 2013; Menichetti et al., 2008). The potential role of inherited faults in the origin of the curved shape of the Southern Andes, however, has never been considered. While ~ N-S oriented normal faults and ~ E-W oriented transfer faults associated to the rifting of the Rocas Verdes basin have been documented affecting the basement of the Patagonian Andes (Fosdick et al., 2011; Likerman et al., 2013), the Jurassic extensional fault array in Tierra del Fuego consist of N to NW oriented normal faults and E to NE oriented transfer faults (Ghiglione et al., 2013). We, therefore, propose that the pre-existing Jurassic faults in the basement of the Southern Andes (N-S trending in the Patagonian Andes, and E-W oriented in the Fuegian Andes) controlled the Late Cretaceous to Cenozoic kinematic evolution and final geometry of the curved Magallanes fold-and-thrust belt.

In our model, during the Middle-Late Jurassic extensional phase associated to the break-up of Pangea and the separation of Antarctica from South America, the southern edge of the South American continent was attenuated by a number of both extensional and transfer faults that mirrored the current shape of the Patagonian Arc (Fig. 8a). This extensional phase was accompanied by the development of a magmatic arc (Patagonian batholith) in the Late Jurassic, and eventually culminated in the opening of the Rocas Verdes marginal basin and Weddell Sea (Fig. 8b). During the closure of the Rocas Verdes basin, the originally straight magmatic arc wrapped around the South American continental margin leading to widespread (~90° to 30°) counterclockwise (CCW) vertical-axis rotations (Rapalini, 2007; Rapalini et al., in press). In the early Late Cretaceous (Fig. 8c), internal contraction of the Rocas Verdes basin and initial deformation of the South American continental margin reactivated the Jurassic faults of the continental basement. In the middle Late Cretaceous (Fig. 8d), collision of the magmatic arc with the attenuated South American continental margin led to the formation of a tectonic domain (central belt) exposing both sedimentary and magmatic units of the Rocas Verdes basin and uplifted blocks of the Paleozoic continental margin (e.g., Cordillera Darwin). Minor CCW tectonic rotations may have still been active at this stage (Rapalini et al., in press). Since the Late Cretaceous-Paleocene the Southern Andes have represented a curved-to-foreland belt, similarly to the rigid indenter models proposed by Ghiglione and Cristallini (2007).

A thick-skinned tectonics affecting the central belt is in agreement with existing models (Menichetti et al., 2008; Torres Carbonell and Dimieri, 2013). Slip partitioning mechanisms along these faulted blocks in the central belt allowed transference of fault-normal compression components into the Magallanes foreland (~N-ward and ~ E-ward contraction in the Fuegian and Patagonian Andes, respectively) throughout the Cenozoic, yielding a radial strain field (Fig. 8e). Following models by Torres Carbonell and Dimieri (2013), we suggest that Cenozoic deformation in the Magallanes fold-and-thrust belt occurred above a décollement at the top of the basement, while compressive stresses were transmitted to the foreland basin by the crustal duplex structures of the central belt (Fig. 8e). Slip partitioning associated to the presence of such faults would have produced widespread sinistral and dextral strike-slip displacements on main thrusts from the internal domains

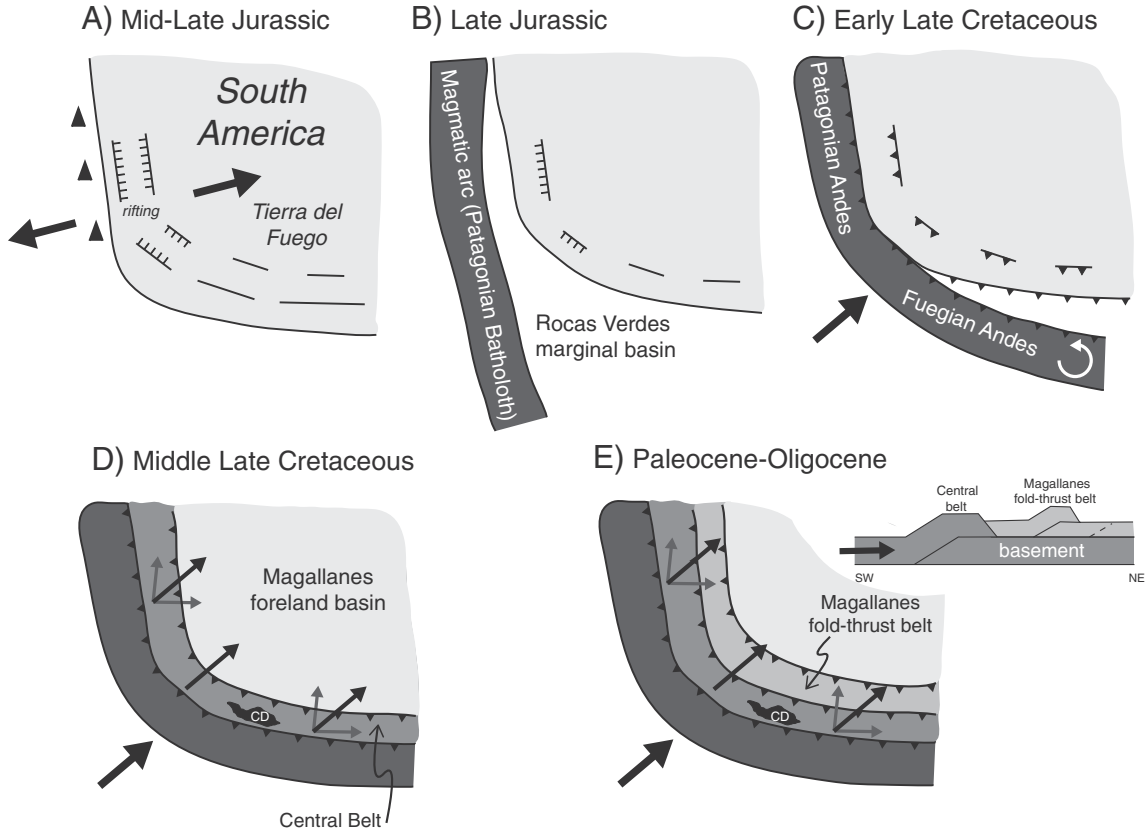

Fig. 8. Proposed kinematic model for the evolution of the Southern Andes. Thick black arrows indicate the direction of the regional strain field. Thin black arrows indicate the displacement vectors of the basement-rooted faulted blocks within the Central Belt; thin grey arrows indicate the fault-normal and fault-perpendicular components resulting from slip partitioning propagating into the Magallanes foreland basin and leading to the formation of the fold-thrust belt.

of the Fuegian and Patagonian Andes, respectively. Further data documenting the existence of such strike-slip tectonics along the Southern Andes are, however, needed to fully test the proposed model.

6.5. An updated definition of the Patagonian Orocline

The curved shape of the Southern Andes inspired Carey (1958) to propose that it may have formed by oroclinal bending of an originally straight orogen. Since then, the curved segment of the Southern Andes has been referred to as the 'Patagonian Orocline'. This initial hypothesis was subsequently supported by sparse paleomagnetic data from the magmatic units, mainly within the internal sectors of the Fuegian Andes, which documented the occurrence of ~90° of counterclockwise rotation (see review by Rapalini, 2007). Tectonic models proposing oroclinal bending in the Cenozoic, related to the opening of the Drake Passage between South America and Antarctica, initially received the largest consensus (Cunningham, 1993; Dalziel et al., 1973; Kraemer, 2003), but were recently challenged by paleomagnetic data from the sedimentary units of the Magallanes fold-and-thrust belt (Maffione et al., 2010; Poblete et al., 2014). Although alternative hypotheses have also emerged, suggesting a primary origin of the curvature of the Southern Andes (Ramos and Aleman, 2000), oroclinal bending models related to the closure of the Rocas Verdes marginal basin in the Late Cretaceous, proposed originally by Burns et al. (1980), represent today a viable mechanism consistent with the known rotation pattern of the Southern Andes (Maffione et al., 2010; Poblete et al., 2014). The regional post-72 Ma 30° CCW rotation of the Fuegian Andes documented by Rapalini et al. (in press), although occurring after complete closure of the Rocas Verdes basin, might still be associated to the tip of this major tectonic process.

The increasing number of paleomagnetic constraints from the Southern Andes suggests that defining the orogenic arc of the Southern Andes as either a primary or a secondary (i.e., orocline) arc is equally inaccurate. Paleomagnetic data from the magmatic and metamorphic units in the outer (Pacific side) part of the orogenic arc consistently show large CCW rotations that support a secondary origin of its curvature. On the other hand, the absence of tectonic rotations in the inner (forelandward) part of the arc, represented by the Magallanes fold-and-thrust belt, indicates that this structure developed during the Cenozoic as a primary arc (Maffione et al., 2010; Poblete et al., 2014). Accordingly, the Patagonian Orocline is more properly formed by the juxtaposition of a secondary and a primary arc, as also suggested by Poblete et al. (2014). For this reason it would be more appropriate to use in the future the term 'Patagonian Arc' when referring to the curved segment of the Southern Andes.

Conclusions

Anisotropy of magnetic susceptibility (AMS) results from weakly deformed Upper Cretaceous to upper Eocene sedimentary rocks from 17 sites within the most internal structural domain of the Magallanes fold-and-thrust belt of Tierra del Fuego (Argentina), reveal a ~ N-S contraction that occurred continuously from the Late Cretaceous until the late Eocene. To reconstruct the evolution of the orogen-scale curvature at the Southern Andes within a wider regional tectonic context, our new and previously published AMS data are integrated, together with available paleomagnetic and fault kinematics constraints. This combined AMS dataset shows that from at least the Early Cretaceous until the end of the Oligocene the tectonic regime at the Southern Andes yielded continuous contraction, variable from ~ E-W in the Patagonian Andes to ~ N-S in the Fuegian Andes, defining a radial strain field.

A direct implication of this study is that the uplift and exhumation of the Cordillera Darwin metamorphic complex occurred within a compressive regional tectonic regime, rather than in extension or strike-slip settings, as alternatively proposed.

In the attempt of explaining the occurrence of a radial strain field in the primary arc of the Magallanes fold-and-thrust belt, and stimulating new research on this topic, we propose a kinematic model whereby reactivation of pre-existing Jurassic faults at the South American margin, oriented sub-parallel to the present-day grain of the orogen, controlled the Late Cretaceous to Cenozoic deformation of the Magallanes foreland basin.

As a final remark, considering the available paleomagnetic constraints from the Southern Andes, we find the broadly used term 'Patagonian Orocline' to be misleading, and propose using the more generic term of 'Patagonian Arc'.

Acknowledgments

This work was funded by Italian *Programma Nazionale di Ricerche in Antartide* (PNRA) funds PROGDEF09-135 awarded to E. Lodolo. We are grateful to M. Gonzáles-Guillot for his support given during the field campaign. MM and DJJvH acknowledge financial support from ERC Starting grant 306810 (SINK) to DJJvH. DJJvH appreciated support through NWO Vidi grant no 864.11.004. Constructive reviews by A. Weil, D. Barbeau and the editor K. Wang greatly helped to improve the quality of the manuscript.

References

Alvarez-Marron, J., McClay, K.R., Harambour, S., Rojas, L., Skarmeta, J., 1993. Geometry and evolution of the frontal part of the Magallanes Foreland Thrust and Fold Belt (Vicuna area), Tierra del Fuego, southern Chile. Am. Assoc. Pet. Geol. Bull. 77 (11), 1904–1921.

Barbeau Jr., D.L., Olivero, E.B., Swanson-Hysell, N.L., Zahid, K.M., Murray, K.E., Gehrels, G.E., 2009. Detrital-zircon geochronology of the eastern Magallanes foreland basin: Implications for Eocene kinematics of the northern Scotia Arc and Drake Passage. Earth Planet. Sci. Lett. 284 (3-4), 489–503.

Biddle, K.T., Uliana, M.A., Mitchum, R.M., Fitzgerald, M.G., Wright, R.C., 1986. The stratigraphic and structural evolution of the central and eastern Magallanes Basin, southern South America. In: Allen, P.A., Homewood, P. (Eds.), Foreland Basins (Special Publication of the International Association of Sedimentologists 8). InBlackwell, Oxford, pp. 41–61.

Borradaile, G., 1987. Anisotropy of magnetic susceptibility: rock composition versus strain. Tectonophysics 138 (2-4), 327–329.

Borradaile, G.J., 1988. Magnetic susceptibility, petrofabrics and strain. Tectonophysics 156 (1-2), 1–20.

Borradaile, G.J., 1991. Correlation of strain with anisotropy of magnetic susceptibility (AMS). Pure Appl. Geophys. PAGEOPH 135 (1), 15–29.

Borradaile, G.J., Tarling, D.H., 1981. The influence of deformation mechanisms on magnetic fabrics in weakly deformed rocks. Tectonophysics 77 (1–2), 151–168.

Borradaile, G.J., Henry, B., 1997. Tectonic applications of magnetic susceptibility and its anisotropy. Earth Sci. Rev. 42 (1-2), 49–93.

Borradaile, G.J., Jackson, M., 2004. Anisotropy of magnetic susceptibility (AMS): Magnetic petrofabrics of deformed rocks. Geological Society Special Publication, pp. 299–360.

Borradaile, G., Keeler, W., Alford, C., Sarvas, P., 1987. Anisotropy of magnetic susceptibility of some metamorphic minerals. Phys. Earth Planet. Inter. 48 (1-2), 161–166.

Bruhn, R.L., 1979. Rock structures formed during back-arc basin deformation in the Andes of Tierra del Fuego. Geol. Soc. Am. Bull. 90 (11), 998–1012.

Bruhn, R.L., Dalziel, I.W.D., 1977. Destruction of the Early Cretaceous marginal basin in the Andes of Tierra del Fuego. Maurice Ewing Ser. 1, 395–405.

Bruhn, R.L., Stern, C.R., De Wit, M.J., 1978. Field and geochemical data bearing on the development of a mesozoic volcano-tectonic rift zone and back-arc basin in southernmost South America. Earth Planet. Sci. Lett. 41 (1), 32–46.

Burns, K.L., Rickard, M.J., Belbin, L., Chamalaun, F., 1980. Further palaeomagnetic confirmation of the magellanes orocline. Tectonophysics 63 (1-4), 75–90.

Calderón, M., Fildani, A., Hervé, F., Fanning, C.M., Weislogel, A., Cordani, U., 2007. Late Jurassic bimodal magmatism in the northern sea-floor remnant of the Rocas Verdes basin, southern Patagonian Andes. J. Geol. Soc. 164, 1011–1022.

Calderón, M., Fosdick, J.C., Warren, C., Massonne, H.J., Fanning, C.M., Cury, L.F., Schwanethal, J., Fonseca, P.E., Galaz, G., Gaytán, D., Hervé, F., 2012. The low-grade Canal de las Montañas Shear Zone and its role in the tectonic emplacement of the Sarmiento Ophiolitic Complex and Late Cretaceous Patagonian Andes orogeny, Chile. Tectonophysics 524–525, 165–185.

Cande, S.C., Leslie, R.B., 1986. Late Cenozoic tectonics of the southern Chile Trench. J. Geophys. Res. 91 (B1), 471–496.

Carey, S.W., 1958. A tectonic approach to continental drift. Continental Drift: A Symposium, pp. 177–355.

Cifelli, F., Mattei, M., Hirt, A.M., Günther, A., 2004. The origin of tectonic fabrics in "undeformed" clays: The early stages of deformation in extensional sedimentary basins. Geophys. Res. Lett. 31 (9), 09601–09604, L09604.

Cifelli, F., Mattei, M., Chadima, M., Hirt, A.M., Hansen, A., 2005. The origin of tectonic lineation in extensional basins: Combined neutron texture and magnetic analyses on "undeformed" clays. Earth Planet. Sci. Lett. 235 (1-2), 62–78.
Cifelli, F., Mattei, M., Rashid, H., Ghalamghash, J., 2013. Right-lateral transpressional tectonics along the boundary between lut and tabas blocks (central iran). Geophys. J. Int. 193, 1153–1165.
Coutand, I., Diraison, M., Cobbold, P.R., Gapais, D., Rossello, E.A., Miller, M., 1999. Structure and kinematics of a foothills transect, Lago Viedma, southern Andes (49°30'S). J. S. Am. Earth Sci. 12 (1), 1–15.
Cunningham, W.D., 1993. Strike-slip faults in the southernmost Andes and the development of the Patagonian orocline. Tectonics 12 (1), 169–186.
Cunningham, W.D., 1994. Uplifted ophiolitic rocks on Isla Gordon, southernmost Chile: implications for the closure history of the Rocas Verdes marginal basin and the tectonic evolution of the Beagle Channel region. J. S. Am. Earth Sci. 7 (2), 135–147.
Cunningham, W.D., 1995. Orogenesis at the southern tip of the Americas: the structural evolution of the Cordillera Darwin metamorphic complex, southernmost Chile. Tectonophysics 244 (4), 197–229.
Cunningham, W.D., Dalziel, I.W.D., Tung-Yi, L., Lawver, L.A., 1995. Southernmost South America-Antarctic Peninsula relative plate motions since 84 Ma: implications for the tectonic evolution of the Scotia Arc region. J. Geophys. Res. 100 (B5), 8257–8266.
Dalziel, I.W.D., 1981. Back-arc extension in the southern Andes: A review and critical reappraisal. Philos. Trans. R. Soc. Lond. 300, 319–335.
Dalziel, I.W.D., 1986. Collision and Cordilleran orogenesis: an Andean perspective. Collision Tectonics 389–404.
Dalziel, I.W.D., Brown, R.L., 1989. Tectonic denudation of the Darwin metamorphic core complex in the Andes of Tierra del Fuego, southernmost Chile: implications for Cordilleran orogenesis. Geology 17, 699–703.
Dalziel, I., Kligfield, R., Lowrie, W., Opdyke, N., 1973. Paleomagnetic data from the southernmost Andes and the Antarctandes. Implications Cont. Drift Earth Sci. 1, 87–101.
Dalziel, I.W.D., De Wit, M.J., Palmer, K.F., 1974. Fossil marginal basin in the southern Andes. Nature 250, 291–294.
Diraison, M., 1998. Evolution cénozoique du Bassin de Magellan et tectonique des Andes Australes. Mém. Doc. Géosci. Rennes 85, 332.
Diraison, M., Cobbold, P.R., Gapais, D., Rossello, E.A., Le Corre, C., 2000. Cenozoic crustal thickening, wrenching and rifting in the foothills of the southernmost Andes. Tectonophysics 316 (1-2), 91–119.
Eagles, G., Livermore, R.A., Fairhead, J.D., Morris, P., 2005. Tectonic evolution of the west Scotia Sea. J. Geophys. Res. B Solid Earth 110 (2), 1–19.
Eichelberger, N., McQuarrie, N., Ehlers, T.A., Enkelmann, E., Barnes, J.B., Lease, R.O., 2013. New constraints on the chronology, magnitude, and distribution of deformation within the central Andean orocline. Tectonics 32 (5), 1432–1453.
Espurt, N., Barbarand, J., Roddaz, M., Brusset, S., Baby, P., Saillard, M., Hermoza, W., 2011. A scenario for late Neogene Andean shortening transfer in the Camisea Subandean zone (Peru, 12° S): Implications for growth of the northern Andean Plateau. Geol. Soc. Am. Bull. 123, 2050–2068.
Esteban, F., Tassone, A., Menichetti, M., Rapalini, A.E., Remesal, M.B., Cerredo, M.E., Lippai, H., Vilas, J.F., 2011. Magnetic fabric and microstructures across the Andes of Tierra del Fuego, Argentina. Andean Geol. 38, 64–81.
Ferré, E., Gleizes, G., Caby, R., 2002. Obliquely convergent tectonics and granite emplacement in the Trans-Saharan belt of Eastern Nigeria: A synthesis. Precambrian Res. 114, 199–219.
Fildani, A., Hessler, A.M., 2005. Stratigraphic record across a retroarc basin inversion: Rocas Verdes-Magallanes Basin, Patagonian Andes, Chile. Bull. Geol. Soc. Am. 117 (11-12), 1596–1614.
Fildani, A., Cope, T.D., Graham, S.A., Wooden, J.L., 2003. Initiation of the Magallanes foreland basin: Timing of the southernmost Patagonian Andes orogeny revised by detrital zircon provenance analysis. Geology 31 (12), 1081–1084.
Fosdick, J.C., Romans, B.W., Fildani, A., Bernhardt, A., Calderón, M., Graham, S.A., 2011. Kinematic evolution of the Patagonian retroarc fold-and-thrust belt and Magallanes foreland basin, Chile and Argentina, 51°30's. Bull. Geol. Soc. Am. 123 (9-10), 1679–1698.
Fosdick, J.C., Grove, M., Hourigan, J.K., Calderón, M., 2013. Retroarc deformation and exhumation near the end of the Andes, southern Patagonia. Earth Planet. Sci. Lett. 361, 504–517.
Fosdick, J.C., Graham, S.A., Hilley, G.E., 2014. Influence of attenuated lithosphere and sediment loading on flexure of the deep-water Magallanes retroarc foreland basin, Southern Andes. Tectonics 33 (12), 2505–2525.
Ghiglione, M.C., 2002. Clastic dykes associated with strike-slip deformation, in synorogenic deposits from the Early Miocene of the Austral basin. Rev. Asoc. Geol. Argent. 57 (2), 103–118.
Ghiglione, M.C., 2003. Estructura y evolución tectónica del Cretácico-Terciario de la costa atlántica de Tierra del Fuego, Estructura y Evolución Tectónica del Cretácico-Terciario de la costa atlántica de Tierra del Fuego (PhD thesis) Ciudad de Buenos Aires (150 pp.).
Ghiglione, M.C., Cristallini, E.O., 2007. Have the southernmost Andes been curved since Late Cretaceous time? An analog test for the Patagonian Orocline. Geology 35 (1), 13.
Ghiglione, M.C., Ramos, V.A., 2005. Progression of deformation and sedimentation in the southernmost Andes. Tectonophysics 405 (1-4), 25–46.
Ghiglione, M.C., Ramos, V.A., Cristallini, E.O., 2002. Fueguian Andes foreland fold and thrust belt: Structure and growth strata. Rev. Geol. Chile 29 (1).
Ghiglione, M.C., Quinteros, J., Yagupsky, D., Bonillo-Martínez, P., Hlebszevtich, J., Ramos, V.A., Vergani, G., Figueroa, D., Quesada, S., Zapata, Y.T., 2010. Structure and tectonic history of the foreland basins of southernmost South America. J. S. Am. Earth Sci. 29 (2), 262–277.
Ghiglione, M.C., Navarrete-Rodríguez, A.T., González-Guillot, M., Bujalesky, G., 2013. The opening of the Magellan Strait and its geodynamic implications. Terra Nova 25, 13–20.
Gombosi, D.J., Barbeau Jr., D.L., Garver, J.I., 2009. New thermochronometric constraints on the rapid Palaeogene exhumation of the Cordillera Darwin complex and related thrust sheets in the Fuegian Andes. Terra Nova 21 (6), 507–515.
Gong, Z., van Hinsbergen, D.J.J., Vissers, R.L.M., Dekkers, M.J., 2009. Early Cretaceous syn-rotational extension in the Organyà basin: new constraints on the palinspastic position of Iberia during its rotation. Tectonophysics 473, 312–323.
González-Guillot, M., Escayola, M., Acevedo, R., 2011. Calc-alkaline rear-arc magmatism in the Fuegian Andes: Implications for the mid-cretaceous tectonomagmatic evolution of southernmost South America. J. S. Am. Earth Sci. 31, 1–16.
Gutiérrez-Alonso, G., Johnston, S.T., Weil, A.B., Pastor-Galán, D., Fernández-Suárez, J., 2012. Buckling an orogen: The Cantabrian Orocline. GSA Today 22 (7), 4–9.
Halpern, M., Rex, D.C., 1972. Time of folding of the yahgan formation and age of the tekenika beds, southern chile, south america. Bull. Geol. Soc. Am. 83 (6), 1881–1886.
Hervé, M., Suarez, M., Puig, A., 1984. The Patagonian batholith S of Tierra del Fuego, Chile: timing and tectonic implications. J. Geol. Soc. 141 (5), 909–917.
Hervé, F., Pankhurst, R.J., Fanning, C.M., Calderón, M., Yaxley, G.M., 2007. The South Patagonian batholith: 150 my of granite magmatism on a plate margin. Lithos 97 (3-4), 373–394.
Hervé, F., Calderón, M., Faúndez, V., 2008. The metamorphic complexes of the Patagonian and Fuegian Andes. Geol. Acta 6 (1), 43–53.
Hrouda, F., 1982. Magnetic anisotropy of rocks and its application in geology and geophysics. Geophys. Surv. 5 (1), 37–82.
Hrouda, F., 1993. Theoretical models of magnetic anisotropy to strain relationship revisited. Phys. Earth Planet. Inter. 77 (3-4), 237–249.
Hrouda, F., Jelinek, V., 1990. Resolution of ferrimagnetic and paramagnetic anisotropies in rocks, using combined low-field and high-field measurements. Geophys. J. Int. 103 (1), 75–84.
Isacks, B.L., 1988. Uplift of the central Andean Plateau and bending of the Bolivian Orocline. J. Geophys. Res. 93 (B4), 3211–3231.
Jackson, M., 1991. Anisotropy of magnetic remanence: A brief review of mineralogical sources, physical origins, and geological applications, and comparison with susceptibility anisotropy. Pure Appl. Geophys. PAGEOPH 136 (1), 1–28.
Jackson, M., Tauxe, L., 1991. Anisotropy of magnetic susceptibility and remanence: Developments in the characterization of tectonic, sedimentary, and igneous fabric. Rev. Geophys. 29 (Suppl.), 371–376.
Jelinek, V., 1977. The Statistical Theory of Measuring Anisotropy of Magnetic Susceptibility of Rocks and Its Application. Geophyzika Brno 88.
Jelinek, V., 1978. Statistical processing of anisotropy of magnetic susceptibility measured on groups of specimens. Stud. Geophys. Geod. 22 (1), 50–62.
Johnston, S.T., Weil, A.B., Gutiérrez-Alonso, G., 2013. Oroclines: Thick and thin. Bull. Geol. Soc. Am. 125 (5-6), 643–663.
Jordan, T.E., Isacks, B.L., Allmendinger, R.W., Brewer, J.A., Ramos, V.A., Ando, C.J., 1983. Andean tectonics related to geometry of subducted Nazca plate. Geol. Soc. Am. Bull. 94 (3), 341–361.
Katz, H.R., 1973. Contrasts in tectonic evolution of orogenic belts in the southwest Pacific. J. R. Soc. N. Z. 3 (3), 333–362.
Klepeis, K.A., 1994. Relationship between uplift of the metamorphic core of the southernmost Andes and shortening in the Magallanes foreland fold and thrust belt, Tierra del Fuego, Chile. Tectonics 13 (4), 882–904.
Klepeis, K.A., Austin Jr., J.A., 1997. Contrasting styles of superposed deformation in the southernmost Andes. Tectonics 16 (5), 755–776.
Klepeis, K., Betka, P., Clarke, G., Fanning, M., Hervé, F., Rojas, L., Mpodozis, C., Thomson, S., 2010. Continental underthrusting and obduction during the Cretaceous closure of the Rocas Verdes rift basin, Cordillera Darwin, Patagonian Andes. Tectonics 29 (3), TC3014. http://dx.doi.org/10.1029/2009TC002610.
Kohn, M.J., Spear, F.S., Dalziel, I.W.D., 1993. Metamorphic P-T paths from Cordillera Darwin, a core complex in Tierra Del Fuego, Chile. J. Petrol. 34 (3), 519–542.
Kohn, M.J., Spear, F.S., Harrison, T.M., Dalziel, I.W.D., 1995. 40Ar/39Ar geochronology and P-T-t paths from the Cordillera Darwin metamorphic complex, Tierra del Fuego, Chile. J. Metamorph. Geol. 13 (2), 251–270.
Kraemer, P.E., 1998. Structure of the Patagonian Andes: Regional balanced cross section at 50°S, Argentina. Int. Geol. Rev. 40 (10), 896–915.
Kraemer, P.E., 2003. Orogenic shortening and the origin of the Patagonian orocline (56° S.Lat). J. S. Am. Earth Sci. 15 (7), 731–748.
Larrasoaña, J.C., Pueyo, E.L., Parés, J.M., 2004. An integrated AMS, structural, palaeo- and rock-magnetic study of Eocene marine marls from the Jaca-Pamplona basin (-Pyrenees, N Spain); new insights into the timing of magnetic fabric acquisition in weakly deformed mudrocks. Geological Society Special Publication, pp. 127–143.
Likerman, J., Burlando, J.F., Cristallini, E.O., Ghiglione, M.C., 2013. Along-strike structural variations in the Southern Patagonian Andes: Insights from physical modeling. Tectonophysics 590, 106–120.
Lodolo, E., Menichetti, M., Tassone, A., Sterzai, P., 2002. Morphostructure of the central-eastern Tierra del Fuego Island from geological data and remote-sensing images. EGS Stephan Mueller Spec. Publ. Ser. 2 (1), 1–16.
Lodolo, E., Menichetti, M., Bartole, R., Ben-Avraham, Z., Tassone, A., Lippai, H., 2003. Magallanes-Fagnano continental transform fault (Tierra del Fuego, southernmost South America). Tectonics 22 (6), 1076. http://dx.doi.org/10.1029/2003TC001500.
Macrì, P., Speranza, F., Capraro, L., 2014. Magnetic fabric of Plio-Pleistocene sediments from the Crotone fore-arc basin: Insights on the recent tectonic evolution of the Calabrian Arc (Italy). J. Geodyn. 81, 67–79.

Maffione, M., Speranza, F., Faccenna, C., 2009. Bending of the Bolivian orocline and growth of the central Andean plateau: Paleomagnetic and structural constraints from the Eastern Cordillera (22-24°S, NW Argentina). Tectonics 28 (4), TC4006. http://dx.doi.org/10.1029/2008TC002402.

Maffione, M., Speranza, F., Faccenna, C., Rossello, E., 2010. Paleomagnetic evidence for a pre-early Eocene (~50 Ma) bending of the Patagonian orocline (Tierra del Fuego, Argentina): Paleogeographic and tectonic implications. Earth Planet. Sci. Lett. 289 (1-2), 273–286.

Maffione, M., Pucci, S., Sagnotti, L., Speranza, F., 2012. Magnetic fabric of Pleistocene continental clays from the hanging-wall of an active low-angle normal fault (Altotiberina Fault, Italy). Int. J. Earth Sci. 101 (3), 849–861.

Maloney, K.T., Clarke, G.L., Klepeis, K.A., Fanning, C.M., Wang, W., 2011. Crustal growth during back-arc closure: Cretaceous exhumation history of cordillera darwin, southern patagonia. J. Metamorph. Geol. 29 (6), 649–672.

Maloney, K.T., Clarke, G.L., Klepeis, K.A., Quevedo, L., 2013. The Late Jurassic to present evolution of the Andean margin: Drivers and the geological record. Tectonics 32 (5), 1049–1065.

Malumián, N., Olivero, E.B., 2006. The cabo domingo group, Tierra del Fuego: Biostratigraphy, paleoenvironments, and events of the marine Eocene-Miocene. Rev. Asoc. Geol. Argent. 61 (2), 139–160.

Malumián, N., Panza, J.L., Parisi, C., Nañez, C., Caramés, A., Torre, E., 2000. Hoja Geológica 5172-III-Yacimiento Río Turbio, provincia Santa Cruz, 1:250.000. Bol. Serv. Geol. Min. Argent. 247 (108 pp.).

Marshak, S., 2004. Arcs, oroclines, salients, and syntaxes - The origin of map-view curvature in fold-thrust belts. In: McClay, K.R. (Ed.)Thrust Tectonics and Petroleum Systems: American Association of Petroleum Geologists Memoir 82, pp. 131–156.

Mattei, M., Sagnotti, L., Faccenna, C., Funiciello, R., 1997. Magnetic fabric of weakly deformed clay-rich sediments in the Italian peninsula: Relationship with compressional and extensional tectonics. Tectonophysics 271 (1-2), 107–122.

Mattei, M., Speranza, F., Argentieri, A., Rossetti, F., Sagnotti, L., Funiciello, R., 1999. Extensional tectonics in the Amantea basin (Calabria, Italy): A comparison between structural and magnetic anisotropy data. Tectonophysics 307 (1-2), 33–49.

Menichetti, M., Lodolo, E., Tassone, A., 2008. Structural geology of the Fuegian Andes and Magallanes fold-and-thrust belt - Tierra del Fuego Island. Geol. Acta 6 (1), 19–42.

Nelson, E.P., 1982. Post-tectonic uplift of the Cordillera Darwin orogenic core complex: evidence from fission track geochronology and closing temperature - time relationships. J. Geol. Soc. 139 (6), 755–761.

Nelson, E.P., Dalziel, I.W.D., Milnes, A.G., 1980. Structural geology of the Cordillera Darwin-collision style orogenesis in the southernmost Andes. Eclogae Geol. Helv. 73 (3), 727–751.

Olivero, E.B., Malumián, N., 1999. Eocene stratigraphy of Southeastern Tierra del Fuego Island, Argentina. Am. Assoc. Pet. Geol. Bull. 83 (2), 295–313.

Olivero, E.B., Malumián, N., 2008. Mesozoic-Cenozoic stratigraphy of the Fuegian Andes, Argentina. Geol. Acta 6 (1), 5–18.

Olivero, E.B., Martinioni, D.R., 2001. A review of the geology of the Argentinian Fuegian Andes. J. S. Am. Earth Sci. 14 (2), 175–188.

Olivero, E.B., Malumián, N., Palamarczuk, S., 2003. Stratigraphy of the Upper Cretaceous-Paleocene from Thetis Bay, Fuegian Andes, Argentina: Tectonic and paleobiologic events. Rev. Geol. Chile 30 (2), 245–263.

Pankhurst, R.J., Riley, T.R., Fanning, C.M., Kelley, S.P., 2000. Episodic silicic volcanism in Patagonia and the Antarctic Peninsula: Chronology of magmatism associated with the break-up of Gondwana. J. Petrol. 41 (5), 605–625.

Parés, J.M., 2004. How deformed are weakly deformed mudrocks? Insights from magnetic anisotropy. Geological Society Special Publication, pp. 191–203.

Parés, J.M., Van der Pluijm, B.A., Dinarès-Turell, J., 1999. Evolution of magnetic fabrics during incipient deformation of mudrocks (Pyrenees, northern Spain). Tectonophysics 307 (1-2), 1–14.

Parés, J.M., Hassold, N.J.C., Rea, D.K., van der Pluijm, B.A., 2007. Paleocurrent directions from paleomagnetic reorientation of magnetic fabrics in deep-sea sediments at the Antarctic Peninsula Pacific margin (ODP Sites 1095, 1101). Mar. Geol. 242, 261–269.

Pastor-Galán, D., Gutiérrez-Alonso, G., Zulauf, G., Zanella, F., 2012. Analogue modeling of lithospheric-scale orocline buckling: Constraints on the evolution of the Iberian-Armorican arc. Bull. Geol. Soc. Am. 124, 1293–1309.

Poblete, F., Roperch, P., Hervé, F., Diraison, M., Espinoza, M., Arriagada, C., 2014. The curved Magallanes fold and thrust belt: Tectonic insights from a paleomagnetic and anisotropy of magnetic susceptibility study. Tectonics 33 (12), 2526–2551.

Prezzi, C.B., Caffe, P.J., Iglesia Llanos, M.P., Orgeira, M.J., 2014. New paleomagnetic data from Upper Oligocene-Lower Miocene rocks of the Northern Argentine Puna-Southern Bolivian Altiplano: Constraining the age of vertical axis rotations. J. Geodyn. 78, 42–52.

Rabinowitz, P.D., Labrecque, J., 1979. The Mesozoic South Atlantic ocean and evolution of its continental margins. J. Geophys. Res. 84 (B11), 5973–6002.

Ramos, V.A., 1989. Andean foothills structures in northern Magallanes basin, Argentina. Am. Assoc. Pet. Geol. Bull. 73 (7), 887–903.

Ramos, V.A., 1999. Plate tectonic setting of the Andean Cordillera. Episodes 22, 183–190.

Ramos, V.A., 2005. Seismic ridge subduction and topography: Foreland deformation in the Patagonian Andes. Tectonophysics 399 (1-4 SPEC. ISS.), 73–86.

Ramos, V.A., Aleman, A., 2000. Tectonic evolution of the Andes, Tectonic Evolution of South America. 31st Int. Geol. Cong., Rio de Janeiro, Brazil, pp. 453–480.

Ramos, V.A., Litvak, V.D., Folguera, A., Spagnuolo, M., 2014. An Andean tectonic cycle: From crustal thickening to extension in a thin crust (34°-37°SL). Geosci. Front. 5 (3), 351–367.

Rapalini, A.E., 2007. A paleomagnetic analysis of the Patagonian orocline. Geol. Acta 5 (4), 287–294.

Rapalini, A.E., Lippai, H., Tassone, A., Cerredo, M.E., 2005. An AMS and paleomagnetic study across the Andes in Tierra del Fuego. 6th International Symposium on Andean Geodynamics (ISAG 2005, Barcelona), Extended Abstracts, pp. 596–599.

Rapalini, A.E., Peroni, J., Luppo, T., Tassone, A., Elena Cerredo, M., Esteban, F., Lippai, H., Vilas, J.F., 2015. Palaeomagnetism of Mesozoic magmatic bodies of the Fuegian Cordillera: implications for the formation of the Patagonian Orocline. In: Pueyo, E.L., Cifelli, F., Sussman, A.J., Oliva-Urcia, B. (Eds.), Palaeomagnetism in Fold and Thrust Belts: New Perspectives. Geological Society, London, Special Publications 425 SP425-3.

Rees, A.I., Woodall, W.A., 1975. The magnetic fabric of some laboratory-deposited sediments. Earth Planet. Sci. Lett. 25, 121–130.

Rochette, P., 1987. Magnetic susceptibility of the rock matrix related to magnetic fabric studies. J. Struct. Geol. 9 (8), 1015–1020.

Rochette, P., Jackson, M., Aubourg, C., 1992. Rock magnetism and the interpretation of anisotropy of magnetic susceptibility. Rev. Geophys. 30 (3), 209–226.

Rossello, E.A., 2005. Kenematics of the Andean sinistral wrenching along the Fagnano-Magallanes Fault Zone (Argentina-Chile Fueguian Foothills). 6th Internation Symposium on Andean Geodynamics, pp. 623–626.

Sagnotti, L., Speranza, F., 1993. Magnetic fabric analysis of the Plio-Pleistocene clayey units of the Sant'Arcangelo basin, southern Italy. Phys. Earth Planet. Inter. 77 (3-4), 165–176.

Sagnotti, L., Faccenna, C., Funiciello, R., Mattei, M., 1994. Magnetic fabric and structural setting of Plio-Pleistocene clayey units in an extensional regime: the Tyrrhenian margin of central Italy. J. Struct. Geol. 16 (9), 1243–1257.

Sagnotti, L., Speranza, F., Winkler, A., Mattei, M., Funiciello, R., 1998. Magnetic fabric of clay sediments from the external northern Apennines (Italy). Phys. Earth Planet. Inter. 105 (1-2), 73–93.

Sagnotti, L., Winkler, A., Montone, P., Di Bella, L., Florindo, F., Mariucci, M.T., Marra, F., Alfonsi, L., Frepoli, A., 1999. Magnetic anisotropy of Plio-Pleistocene sediments from the Adriatic margin of the northern Apennines (Italy): Implications for the time-space evolution of the stress field. Tectonophysics 311 (1-4), 139–153.

Sintubin, M., 1994. Clay fabrics in relation to the burial history of shales. Sedimentology 41 (6), 1161–1169.

Somoza, R., Ghidella, M.E., 2005. Convergence in the western margin of South America during the Cenozoic: Subduction of Nazca, Farallon and Aluk plates. Rev. Asoc. Geol. Argent. 60 (4), 797–809.

Somoza, R., Ghidella, M.E., 2012. Late Cretaceous to recent plate motions in western South America revisited. Earth Planet. Sci. Lett. 331–332, 152–163.

Somoza, R., Zaffarana, C.B., 2008. Mid-Cretaceous polar standstill of South America, motion of the Atlantic hotspots and the birth of the Andean cordillera. Earth Planet. Sci. Lett. 271 (1-4), 267–277.

Soto, R., Larrasoaña, J.C., Arlegui, L.E., Beamud, E., Oliva-Urcia, B., Simón, J.L., 2009. Reliability of magnetic fabric of weakly deformed mudrocks as a palaeostress indicator in compressive settings. J. Struct. Geol. 31 (5), 512–522.

Speranza, F., Sagnotti, L., Mattei, M., 1997. Tectonics of the Umbria–Marche–Romagna Arc (central northern Apennines, Italy): new paleomagnetic constraints. J. Geophys. Res. 102, 3153–3166.

Stern, C., DeWitt, M., 2004. Rocas Verdes ophiolites, southern South America: remnants of progressive stage of development of oceanic-type crust in a continental margin back-arc basin. In: Diley, Y., Robinson, P. (Eds.), Ophiolites on Earth History vol. 218. Geological Society, London (Sp. Pub.), pp. 665–683.

Tarling, D.H., Hrouda, F., 1993. The Magnetic Anisotropy of Rocks. Chapman, Hall, London (217 pp.).

Thomson, S.N., 2002. Late Cenozoic geomorphic and tectonic evolution of the Patagonian Andes between latitudes 42°S and 46°S: An appraisal based on fission-track results from the transpressional intra-arc Liquiñe-Ofqui fault zone. Bull. Geol. Soc. Am. 114, 1159–1173.

Thomson, S.N., Hervé, F., Stökhert, B., 2001. Mesozoic-Cenozoic denudation history of the Patagonian Andes (Southern Chile) and its correlation to different subduction processes. Tectonics 20 (5), 693–711.

Torres Carbonell, P.J., Olivero, E.B., 2012. Sand dispersal in the southeastern Austral Basin, Tierra del Fuego, Argentina: Outcrop insights from Eocene channeled turbidite systems. J. S. Am. Earth Sci. 33, 80–101.

Torres Carbonell, P.J., Dimieri, L.V., 2013. Cenozoic contractional tectonics in the Fuegian Andes, southernmost South America: A model for the transference of orogenic shortening to the foreland. Geol. Acta 11 (3), 331–357.

Torres Carbonell, P.J., Olivero, E.B., Dimieri, L.V., 2008. Structure and evolution of the Fuegian Andes foreland thrust-fold belt, Tierra del Fuego, Argentina: Paleogeographic implications. J. S. Am. Earth Sci. 25 (4), 417–439.

Torres Carbonell, P.J., Dimieri, L.V., Olivero, E.B., 2011. Progressive deformation of a Coulomb thrust wedge: The eastern Fuegian Andes Thrust-Fold Belt. Geological Society Special Publication, pp. 123–147.

Torres Carbonell, P.J., Dimieri, L.V., Martinioni, D.R., 2013. Early foreland deformation of the Fuegian Andes (Argentina): Constraints from the strain analysis of Upper Cretaceous-Danian sedimentary rocks. J. Struct. Geol. 48, 14–32.

van Hinsbergen, D.J.J., Zachariasse, W.J., Wortel, M.J.R., Meulenkamp, J.E., 2005. Underthrusting and exhumation: A comparison between the External Hellenides and the 'hot' Cycladic and 'cold' South Aegean core complexes (Greece). Tectonics 24, TC2011. http://dx.doi.org/10.1029/2004TC001692.

Weil, A.B., Sussman, A.J., 2004. Classification of curved orogens based on the timing relationships between structural development and vertical-axis rotations. In: Sussman, A.J., Weil, A.B. (Eds.), Paleomagnetic and Structural Analysis of Orogenic Curvature. Spec. Pap. Geol. Soc. Am. 383, pp. 1–17.

Weil, A.B., Yonkee, A., Sussman, A., 2010. Reconstructing the kinematic evolution of curved mountain belts: A paleomagnetic study of Triassic red beds from the Wyoming salient, Sevier thrust belt, U.S.A. Bull. Geol. Soc. Am. 122, 3–23.

Wilson, T.J., 1991. Transition from back-arc to foreland basin development in the southernmost Andes: stratigraphic record from the Ultima Esperanza District, Chile. Geol. Soc. Am. Bull. 103 (1), 98–111.

Winslow, M.A., 1981. Mechanisms for basement shortening in the Andean foreland fold belt of southern South America. Geol. Soc. Spec. Pub. 9, 513–528.

Winslow, M.A., 1982. The structural evolution of the Magallanes Basin and neotectonics in the southernmost Andes, Antarctic geoscience. 3rd symposium on Antarctic geology and geophysics, Madison, August 1977, pp. 143–154.

Yonkee, A., Weil, A.B., 2010. Reconstructing the kinematic evolution of curved mountain belts: Internal strain patterns in the Wyoming salient, Sevier thrust belt, U.S.A. Bull. Geol. Soc. Am. 122, 24–49.